OT4LAKE KIVU

Assessment and Monitoring of Soil Erosion Parameters in the Transboundary Lake Kivu and Ruzizi River Basin

February 2022

Dr. Stefanie Feuerstein, Zhiyuan Wang and Dr. Felix Bachofer
German Aerospace Center - German Remote Sensing Data Center (DLR-DFD)
Mu¨nchener Str. 20
81241 Wessling Germany

Co-funded by the European Union

SUBMITTED BY:

Contents

Executive Summary

In the EO4Lake Kivu project, earth observation data is used to assess the ability to analyse erosion risk from a satellite perspective. With this, the EO4Lake Kivu project supplements the analysis performed in the course of the *Baseline Study for the Basin of Lake Kivu and Ruizizi River* (*Sher Consult*, 2020) including the herein performed RUSLE simulations. The scientific work of the EO4Lake Kivu project is divided into four work packages (WP). WP1 and WP2 analyze the parameters vegetation dynamics and extreme precipitation events. These two parameters are combined into an erosion risk index. The results show that there are regions with seasonally repeating low vegetation cover reflected by a low NDVI. This especially applies to agricultural fields and grasslands as identified by the comparison of the NDVI with ESA's WorldCover map. Particularly low vegetation cover is regularly found in the Ruzizi plain and the southern slopes of the vulcanoes in the north of the study area, where the main agricultural fields are found.

In the precipitation analysis not a single hot-spot month or region could be determined. However, an increased in the number of extreme events is detected for the months April or May, August and November or December in most years. By bringing the vegetation dynamics and extreme precipitation events together, the erosion risk for each season of the years 2016-2020 is identified. Erosion risk hot-spots differ from year to year and from season to season. Nevertheless, some high risk areas could be identified: The Ruzizi plain, the area between the city of Goma and the northern volcanic region, the city agglomerations of Goma and Bukavu and the grasslands east of lake Kivu. A comparison of the satellite based erosion risk analysis and the results of the RUSLE simulation show that both approaches come to similar results (although some hot-spots do not completely align in their location and extend). This suggests that both approaches can be used complementary.

In WP 4, turbidity data of lake Kivu is used to determine, if high erosion risk leads to an increased lake turbidity due to increased sediment input. The quantitative comparison of erosion risk and turbidity does not show a clear connection between the two parameters. This is likely due to the short temporal and small spatial extend of a turbidity increase subsequent to soil erosion events. The turbidity increase may only be visible for the river deltas and may not affect the lake water further away from the coast. A closer look at turbidity information near the coastline and in a higher temporal resolution may lead to more supportive results.

WP 5 analyses another erosion risk parameter: the population growth. By using the World Settlement Footprint, the growth of the two city agglomerations of Goma and Bukavu is analyzed. Especially Goma shows a strong growth in city area from 1995 to 2005. For Bukavu, only minor growth is shown in the last decades. This is probably due to the rugged terrain around the city which does not allow for intense growth outside the city outlines. The growth between 1995 and 2015 depicted by the World Settlement Footprint is used as one input parameter for the SLEUTH model, with which the growth of these

two agglomerations until 2050 is simulated. The predicted urban growth shows only a small increase in city area for Bukavu. Still, this is likely to be a result of the steep slopes around the city. For Goma, a stronger growth of the city area is predicted, especially along the road network on the Rwandan side of the agglomeration. All in all one can expect a growth of the cities in the study area, leading to an increase in population, an increase of sealed surfaces leading to stronger surface runoff of precipitation and a higher demand for agricultural products. These factors are likely to further increase the pressure on the soils in the study area and can provoke more intense soil erosion and soil degradation.

The EO4Lake Kivu project shows, how satellite data can be used to identify erosion hot-spots over a large area. The results suggest that soils are endangered in the area. Threats are unsuitable land use /agriculture practices leading to temporally low vegetation cover. An increase in population can further increase the pressure on the available land surfaces. However, the analysis also shows how efficient nature conservation measures can protect lands from soil erosion. The large protected areas in the region show very low erosion risk throughout the year due to year-round dense vegetation cover - a result that was found by both, the remote sensing analysis and the RUSLE simulation.

1. Introduction

Healthy soils are the basis of functioning ecosystems. They are habitats for a large number of microorganisms and for a diversity of animals and plants and the basis of a productive agriculture. However, global soils are endangered by degradation. In their *Main Report on the Status of the World's Soil Resources*, the FAO states, that land degradation is believed to be expanding in an alarming rate, especially in Africa, where 65% of the soils on agricultural lands have become degraded since the middle of the twentieth century (*FAO and ITPS*, 2015). The most widespread cause of soil degradation for African soils is water erosion (*FAO and ITPS*, 2015). This is particularly true for the area around the Equator, which is named in the top three hot spot regions that show strongest and most intense erosion in the world (*Borrelli et al.*, 2017).

The lake Kivu and Ruzizi river basin is located in this area at the trans-boundary region of the Republic of Burundi, the Democratic Republic of Congo and the Republic of Rwanda and is characterized by a mountainous terrain ranging between 1400 m and more than 4000 m in altitude. This ruggedness of the terrain increases its natural erosion risk. Another reason, why the area is endangered by soil erosion are the changes in land cover, mainly through the transformation from natural vegetation to agricultural lands or built-up areas in the last decades. *Karamage et al.* (2016) have shown that land use change in Rwanda, one of the densest populated countries in eastern Africa, have led to a decrease of 64.5% and 31.1% in forest and grasslands cover, respectively, between 1990 and 2016. Especially after 2010, the observed deforestation rate was nearly twice as high as it was in 1990. The loss in natural land covers can mainly be explained by an increase in cropland and built-up area (134% and 304% between 1990 and 2016, respectively). Through this shift in land cover towards unsuitable land use and land cover types, strong erosion is caused in the catchment area of Lake Kivu (*Akayezu et al.*, 2020).

Besides topsoil destabilization, an increase in surface runoff through land use changes and a change in the regional precipitation pattern are factors that lead to an increase in soil erosion (*Karamage et al.*, 2016). For the area of lake Kivu, only a slight increase in annual precipitation is projected for the future. However, the inner annual precipitation pattern is likely to change significantly. According to IPCC scenarios, an increase of November, December and January precipitation between 11% and 19% is likely for the region together with a decrease in precipitation of around 2% in July (*Sher Consult*, 2020). To understand how the changes in precipitation pattern and in land cover influence soil erosion in the region of lake Kivu, a principal understanding of the current erosion risks and activities is needed.

The Lake Kivu and Ruzizi River Basin Authority (ABAKIR), which was established by the three countries in the area of lake Kivu and Ruzizi Basin, the Republic of Burundi, the Democratic Republic of Congo and the Republic of Rwanda, engages in the integrated management of water resources in the lake Kivu and Ruzizi River Basin. For this, the

Baseline Study for the Basin of Lake Kivu and Ruizizi River (*Sher Consult*, 2020) collects relevant information on the area. It is funded within the GIZ (Deutsche Gesellschaft für Internationale Zusammenarbeit GmbH) project "Support for the integrated management of the water resources of Lake Kivu and the Ruzizi River". The baseline study includes detailed information on the administrative and socio-economic and the physical and climatologic context, on water resources, land use and ecosystems and on environmental and natural hazards in the region. It also includes an investigation on soil degradation. For this, the Revised Universal Soil Loss Equation (RUSLE) model was used to estimate soil erosion quantities with the aim of estimating soil losses and to identify areas of risk to enable the development of soil conservation measures. The project EO4Lake Kivu complements this analysis by the use of time-series of earth observation (EO) data. With this, a supplement analysis is performed to further identify erosion risk hot-spots and parameters in the region in the region.

2. Study Area

A detailed description of the study area can be found in the *Baseline Study for the Basin of Lake Kivu and Ruizizi River* (*Sher Consult*, 2020). In this report, only a brief description on the most important features to which is made reference in this project, will be carried out. Figure 2.1 shows an overview of the study area. The outline of the Lake Kivu and Ruzizi Basin coincides with the outline of the area considered in the baseline study and its including RUSLE model area.

The map also shows the outlines of the sub-basins located within the study area. These sub-basins are derived from the HydroBASINS level 8 data set (*Lehner and Grill*, 2013). In the study area, there are 25 sub-basins. The northern ones have their main outflow into lake Kivu. The central basins have their main outflow into the Ruzizi river and from there into lake Tanganyika. The southern sub-basins directly water into lake Tanganyika. At the northern end of the study area, a very high mountain range is located, which consists of a number of active and inactive volcanoes. Particularly interesting for the presented analysis are the vulcanoes Nyiragongo, Nyamuragira and Karisimbi with heights of up to more than 4000 m a.s.l. and recorded volcanic activity in the last centuries. Other mountainous regions can be found in the southwest and southeast of the study area, the latter one being mainly covered by forest and protected as Nyungwe Forest on the Rwandan side and Kibira National Park on the Burundi side. Between lake Kivu and lake Tanganyika, the Ruzizi River Plain is located, which was formed by the Ruzizi River that connects the two lakes. This plain is an important agricultural region in the area.

The cities of Goma and Bukavu are located at the northern and the southern coast of lake Kivu in the Democratic Republic of Congo. These two cities and their surrounding agglomerations will be the focus of the urban growth simulations performed in chapter 9.

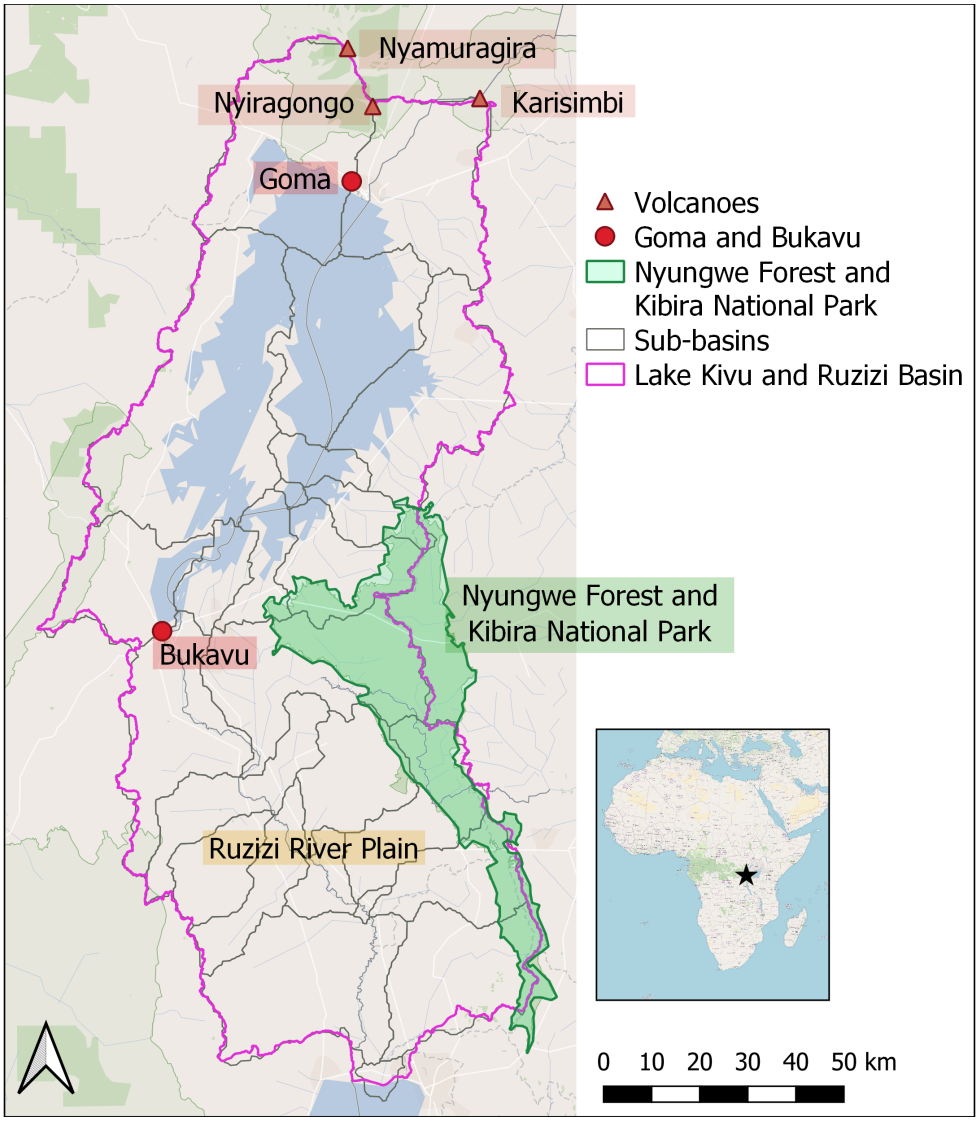

2.1 Study area and location of important features mentioned in the data analysis.

3. Research Activity and Work Packages

The scientific work is structured in 4 work packages (WP). WP 1 to WP 3 use EO data to analyze the erosion risk in the area and to identify regions that can be considered *high erosion risk hot-spots*. For this, WP 1 focuses on the analysis of vegetation dynamics by taking advantage of long time series of NDVI information. Long-term vegetation changes of the last two decades are analyzed together with seasonal and interanual cycles of the vegetation cover. Furthermore, the vegetation cover is compared to land use information to identify those land cover types that lead to a strong variability in vegetation cover over time and especially to phases with sparse cover or open soil.

WP 2 analyses the precipitation pattern in the region, which is the second parameter considered to quantify erosion risk. The precipitation analysis uses a daily product to identify the seasonal precipitation distribution as well as strong precipitation events. These strong events are able lead to strong surface runoff and with this to provoke soil erosion. The analyses of WP 1 and WP 2 are combined to detect those areas and time periods, for which low vegetation cover and an increased number in strong precipitation coincide. The combination of the two factors results in an erosion risk map that is produced on a monthly scale for the years 2016 to 2020. In WP 3 lake turbidity data is used to test, whether increased erosion risk is reflected by an increased sediment intake into lake Kivu and with this leads to an increase in turbidity of the lake water.

WP 4 focuses on an indirect factor for soil erosion risk: the change in urbanization of two city agglomerations in the area, i.e. Bukavu in the south and Goma north of lake Kivu. The population growth of the last decades is analyzed using the World Settlement Footprint (*Marconcini et al.*, 2020), an EO based urbanization data set. Further, the projected city growth until 2050 is simulated using an urban growth model.

4. Work Package 1: Analysis of Vegetation Dynamics

The vegetation dynamics play an important role in the erosion risk estimation. NDVI products have been used in previous studies to analyze erosion risks, e.g, in *Hazarika and Kiyoshi* (2001) and *Sharma* (2010). Bare soil or soil that is covered by sparse vegetation is a lot more affected by soil erosion than soil that is covered by dense vegetation. In the first step of the vegetation analysis, an NDVI product is used to identify areas and periods with low vegetation cover that are prone to soil erosion. In a second step, the NDVI is compared to land use data to identify land covers that lead to low NDVI values.

4.1. NDVI analysis

4.1.1. MODIS NDVI Data

For the analysis of long-term vegetation dynamics, the MODIS NDVI Version 6.1 products MOD13Q1 (*Didan*, 2021a) derived from MODIS Terra, and MYD13Q1 (*Didan*, 2021b) derived from MODIS Aqua, are used. These products are available for the whole lifetime of the two satellites Terra and Aqua, which were launched in 2000 and 2002, respectively. The data sets have a temporal resolution of 16 days and a spatial resolution of 250 m. For each product, the best available pixel value from all acquisitions of the previous 16 day period is used. Two vegetation layers are delivered with each product: the NDVI and EVI vegetation indices. In the presented analysis, we exclusively make use of the NDVI index. A reason to focus on the NDVI is its high temporal resolution and the long time period that is covered by these two products. Furthermore, the NDVI index has a proven robustness

and reliability to monitor vegetation dynamics, also in the eastern African region where the study area is located (e.g. *La*, 2013; *Landmann and Dubovyk*, 2014; *Musau et al.*, 2018).

The 16-days product is downloaded from the NASA EarthData platform. From here, files are retrieved in hdf-format and in the sinusoidal projection, which is typical for MODIS data products. The granule h20v09 covers the whole study area. In a first step, the data is reprojected to geographic projection (EPSG: 4326) and transformed into geotiff-format. The data comes with a quality layer. This quality layer gives information on marginal data and pixels that cover snow/ice or clouds. In the case of the lake Kivu project, the quality layer is used to mask marginal data and clouds from the NDVI product.

The cloud-flagged high quality data is then used to extract all long-term vegetated surfaces. Like this, only those pixels are used for the analysis, which cover vegetated areas and surfaces like water, rocks, build-up area etc are excluded. For this, an approach is used that has been applied in a number of other studies, e.g. *Detsch et al.* (2016), *Sarmah et al.* (2018) or *Eastman et al.* (2013): Over the full time period of 20 years (2001-2020), the mean NDVI is calculated and those areas are masked, for which the long-term NDVI is below 0.15. These areas are considered non-vegetated on a long-term scale and are not relevant for the analysis of vegetation dynamics. The remaining vegetated surfaces of the years 2001 to 2020 are then aggregated to monthly NDVI indices on a hexagonal grid with the size of 0.25°. Through this aggregation, a more generalized and quantitative look on the vegetation dynamics is possible than when performing a pixel-by-pixel analysis (compare *Jurasinski and Beierkuhnlein* (2006)).

4.1.2. Long-term Vegetation Changes

The long time series of MODIS allows for the analysis of long-term vegetation dynamics. For this, the full period is divided into four sub-periods: P1 (2001-2005), P2 (2006-2010), P3 (2011-2015) and P4 (2016-2020). For each of the periods, a long-term median image is created from the monthly medians. The result is presented in the upper part of figure 4.1. It shows the five-year median of each period P1-P4. The highest and most robust NDVI values throughout all four periods can be observed for the southeastern region of the study area where the Nyungwe Forest (Rwanda) and the Kabiri national park (Burundi) are located. In the plains of Ruzizi River in the southern study area, lower NDVI values around 0.5-0.6 can be observed. This is due to the agricultural fields found in the area, for which vegetation cover is low during and after harvesting phases. In the northern part of the study area around lake Kivu, where the topography is more extreme, lower NDVI values can be observed. To visualize how vegetation cover changed over time, the lower part of figure 4.1 shows the vegetation change from each period to its following period. Red color indicates a decrease in vegetation cover while green color shows an increase.

Especially in the northern part of the study area north of the city of Goma, a strong decrease of vegetation cover can be observed, especially from P1 to P2. This area is marked by an extreme topography and coincides with the location of Nyamulagira, Nyiragongo and Mount Karisimbi volcanoes with elevations that exceed 4500 m a.s.l.. Especially the

volcanoes Nyamuragira and Nyiragongo have experienced strong activities in the time period covered in the analysis. The decline in vegetation cover in the area of Nyamuragira from P1 to P2 and from P2 to P3 can be explained by volcanic eruptions in the years 2006, and 2010 and 2011, for which lava flows were localized in this area by *Head et al.* (2013).

South of the volcanic region at the northern end of Lake Kivu, there is another area, for which a decline in vegetation can be observed over the whole time period. This decline coincides with the city agglomeration of Goma and can be explained by the growth of the city agglomeration. This topic will be further discussed in chapter 9 - however, the urban growth depicted by figure 9.2 aligns with the decrease in vegetation cover.

In the southeastern part of the study area, where the Nyungwe Forest (Rwanda) and Kibira national park (Burundi) area is located, there are losses in vegetation cover at the border of the preservation areas from P2 to P3 - these losses may be due to forest clearing in the buffer zones of the national park as described by *Kayiranga et al.* (2016) and *Rutebuka et al.* (2018). Fortunately an increase in NDVI from P3 to P4 can be observed for the Kibira national park.

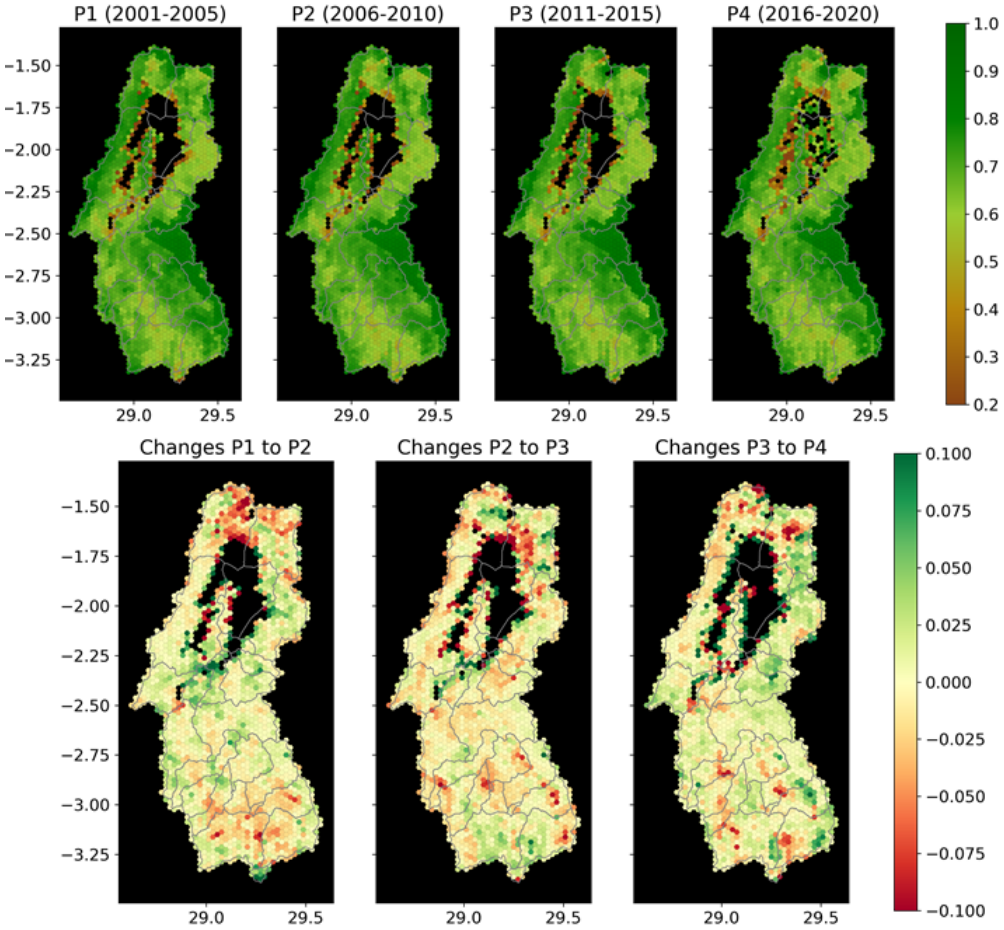

4.1 Long-term vegetation analysis. Top: Median of five-year periods on hexagonal grid of 0.25°. Below: Change between periods.

4.1.3. Seasonal Vegetation Dynamics

To more closely analyze the seasonal and inter-annual vegetation cycle and to find surfaces that are vulnerable to soil erosion, a closer look is taken at period P4 from 2016 to 2020. Due to the high cloud coverage in this area for parts of the year, data availability is limited in some months, even though the MODIS satellites cover the area (almost) daily. This is why, the inner-annual analysis of the vegetation dynamics is performed on a seasonal level. For this, the year is split into wet and dry season. The wet season covers the months January to May and September to December while the dry season covers June to August. The short dry season in January is not taken into account here.

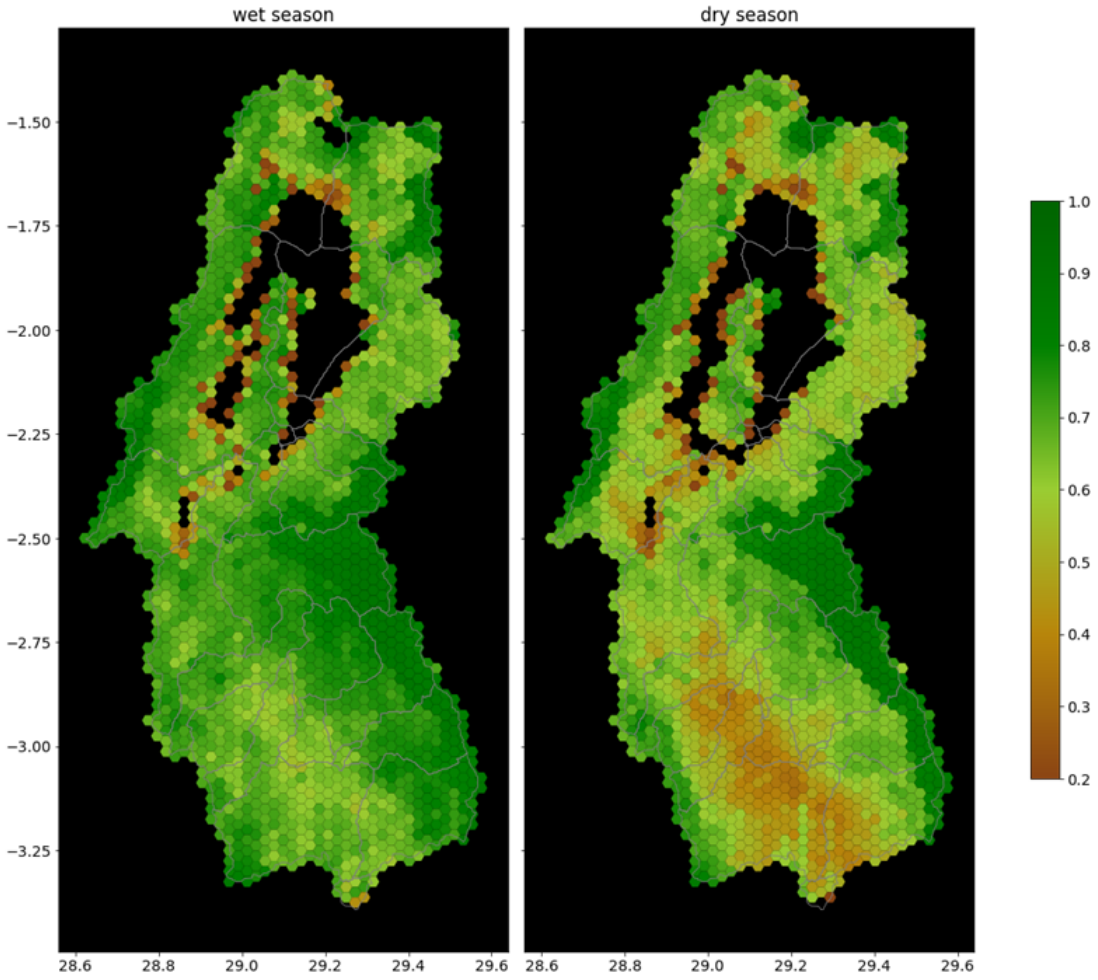

4.2 NDVI median of 2016-2020 for the dry and wet season.

As can be noted from figure 4.2, the NDVI is much lower for the dry season, especially for the region of the Ruzizi plain. Along the coast line of lake Kivu, low vegetation cover can be observed for both, the wet and the dry season. The main reason for this is probably the aggregation of water and land pixels within one hexagon, but may also partly be due to human activity, build-up area or the movement of the lake coastline.

This median seasonal NDVI is further calculated for each year from 2016 to 2020. Figure

4.3 shows the median NDVI for dry and wet seasons in 2016, while the respective plots for the other years can be found in the appendix chapter A.1. There is data available for almost the entire study area for each year. However, there are regions for each season of each year, for which no data is available from the MODIS NDVI data. The lowest data coverage is found in the mountainous regions in the volcanic north and the south-eastern mountain ridge where a lot of cloud cover or marginal data quality occur. The seasonal NDVI information of each year is later, together with the precipitation, used to estimate the erosion risk on a spatio-temporal scale.

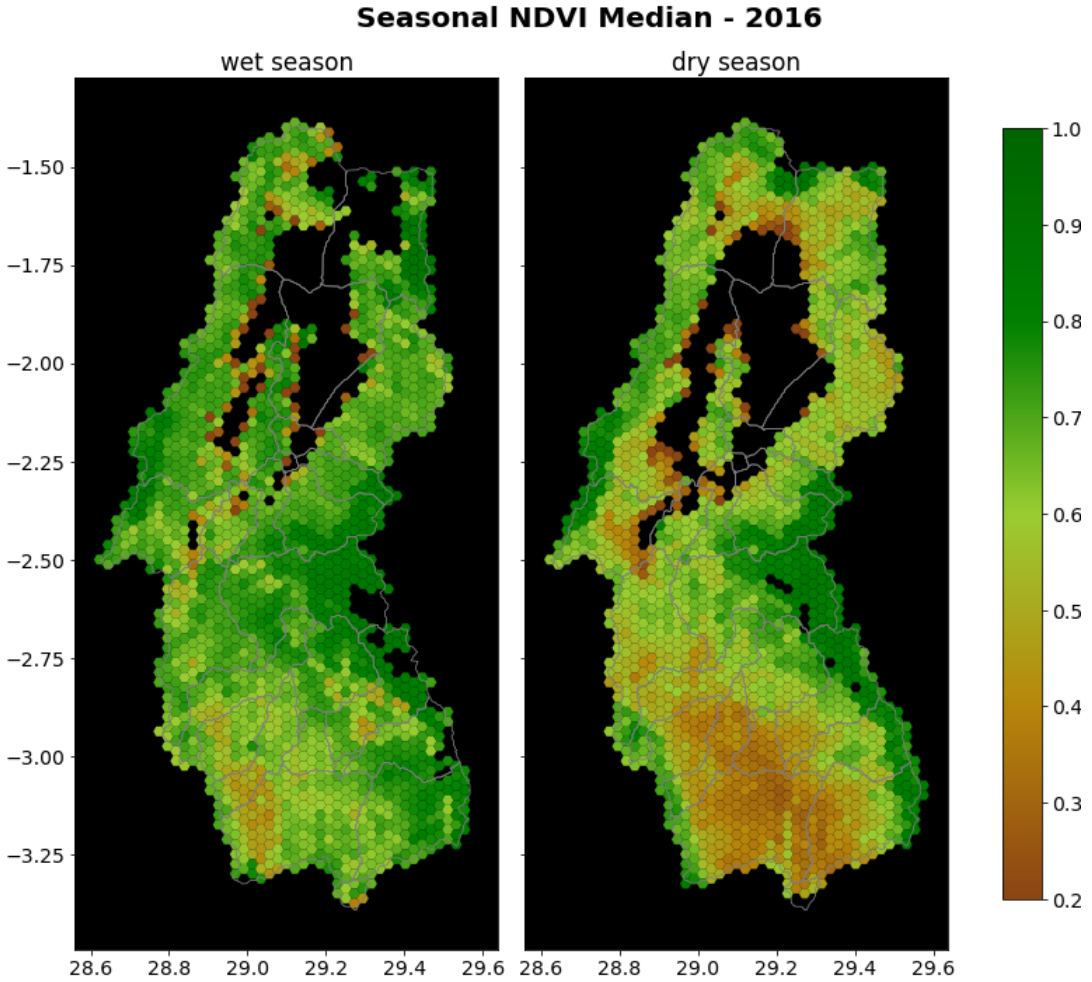

4.3 NDVI median of 2016 for the dry and wet season.

4.2. Copernicus Land Cover information

4.2.1. ESA's WorldCover map

In October 2021, ESA released their new WorldCover map (*Zanaga et al.*, 2021). The WorldCover map shows the land cover of 2020. It is based on SAR data and optical

remote sensing data of the two satellites Sentinel-1 and Sentinel-2. It is a freely accessible, global product in 10 m resolution and offers 10 land cover classes and a minimum overall accuracy of 75%.

On the right panel of figure 4.4, the 10 m land cover is plotted for the lake Kivu study area. The large forests of the national parks in the southeast are clearly visible on the map. Further, cropland is detected along the Ruzizi river and south of lake Kivu. Intense agricultural land use is also found for the southwestern hillside of the Karisimbi volcano northeast of lake Kivu. Most of the Ruzizi river plain that is not used for agriculture, is covered by grass- and shrubland. Clearly visible are the city agglomerations of Goma (north of lake Kivu) and Bukavu (south of the lake). More larger settlements are located along the Ruzizi river.

The WorldCover data is used to identify surfaces, which show a low vegetation cover (with an NDVI below 0.5) during wet or dry season. These surfaces are likely to be endangered by soil erosion. The left panel of figure 4.4 combines the NDVI analysis of the previous sections with the land cover information: For the wet and dry seasons of each year between 2016 and 2020, the land cover is identified that falls into hexagons with an NDVI below 0.5.

The figure shows that during wet season, the two land cover classes that mostly lead to low NDVI values are permanent water bodies (57%) and grassland (23%). It is not surprising that the lowest NDVI values are found for the water class when looking at figure 4.2, which shows the five-year median NDVI. Many of the hexagons along the coast of lake Kivu show a very low NDVI value. This is probably due to the size of the hexagons and the resulting mixture of water and land pixels within the hexagon. Further comparison of the seasonal median NDVI with land cover classes shows that most of the grasslands that have a low NDVI value during wet season are located in the Ruzizi plain.

During dry season, the two most important land cover classes that lead to an NDVI below 0.5 are grassland (47%) and cropland (35%). This is a result of the low NDVI during dry season in the Ruzizi plain, but also around and north of lake Kivu, where most of the grass- and croplands are found.

Besides the herbacious wetland class, which is very rare in the whole study area, shrubland and forested areas are the ones with lowest share of NDVI values below 0.5 for both, wet and dry season. For shrubland this is probably due to its overall low abundance in the study area, while for the evergreen forest, year-round large NDVI values are found.

The main results of the land cover analysis are not surprising: Forests show a high NDVI value troughout the year which is likely to significantly reduce the erosion risk. During wet season, low NDVI may be found along the coasts of the lake but also for grasslands, which do not show a vegetation cover as dense as other land covers. Especially during dry season, this vegetation density or at least the greenness of these surfaces strongly decreases due to water availability. Further, croplands show a strong decrease in NDVI from wet to dry season due to the harvesting of the fields and the drying out of field crops, again a result of low water availability.

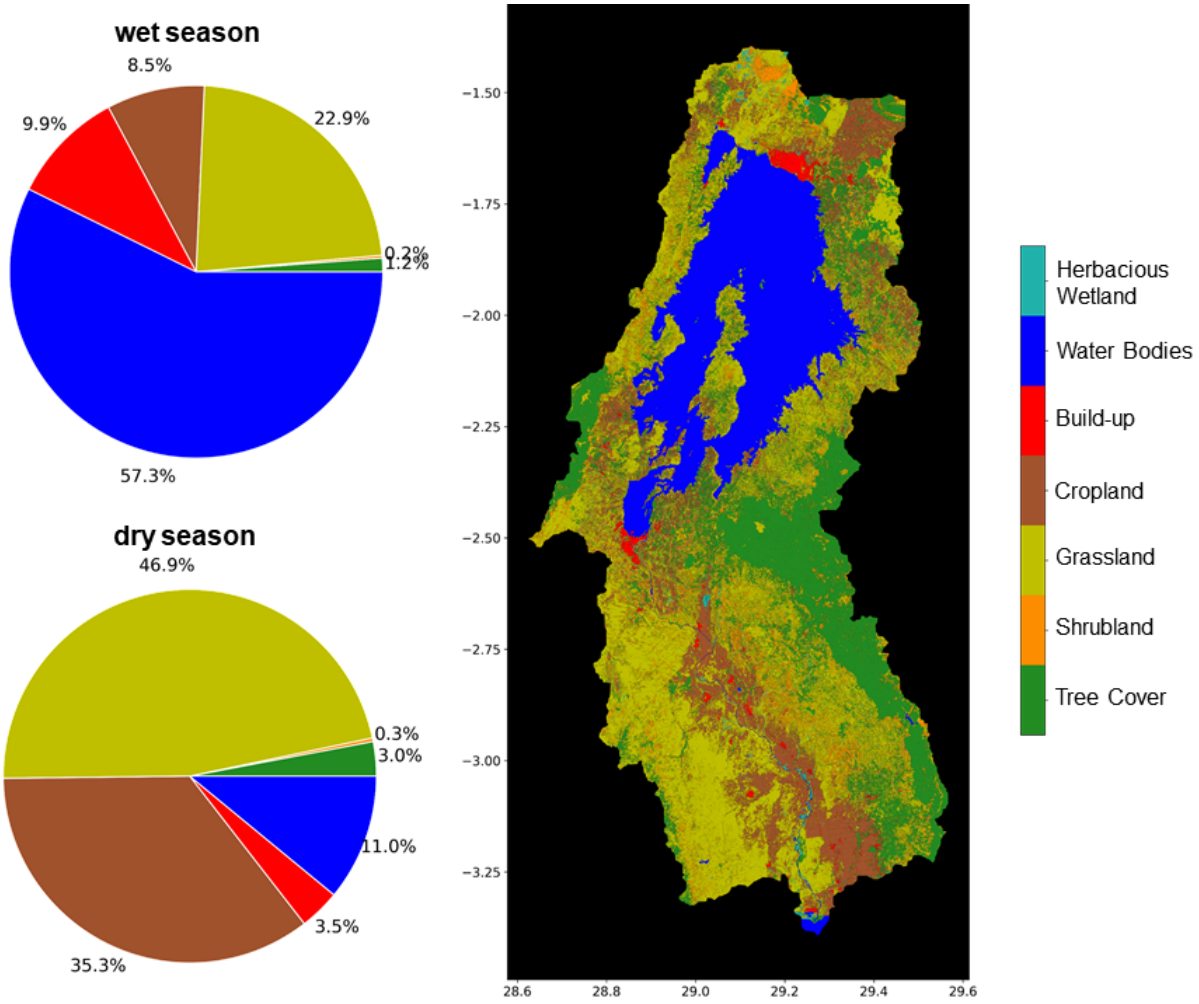

4.4 Land cover map for the lake Kivu study area based on ESA's WorldCover map (right) and land use classes with NDVI below 0.5 for wet and dry season of 2016-2020 (left).

5. Work Package 2: Precipitation Analysis

5.1. CHIRPS Version 2.0 data

To analyze the spatio-temporal distribution of precipitation in the study area, the Climate Hazards Group InfraRed Precipitation with Station Data (CHIRPS) v2.0 dataset is used (*Funk et al.*, 2015). The data can be downloaded from `https://data.chc.ucsb.edu/products/CHIRPS-2.0/` and comprises a more than 40 years long (from 1981 to present) quasi-global (from 50°S to 50°N) rainfall data set. It is available in a 0.05°spatial resolution and in a daily, pentadal and monthly temporal resolution. The dataset is a synthesis of satellite derived and in-situ data. Its consistency has been validated and used by a number of studies that cover eastern Africa (e.g. *Dinku et al.*, 2018; *Muthoni et al.*, 2019). In this analysis, the daily product is used since it enables to identify short term strong

precipitation events.

5.2. Mean Annual Precipitation Sums

Figure 5.1 shows the monthly mean precipitation sums for P4 (2016-2020) divided into months assigned to wet (September to May) and dry seasons (June,July, August). As can be seen from the figure, the monthly mean precipitation is 10-100 times higher during the wet season compared to the dry season. Especially in the mountainous regions of the study area in the southeast and southwest as well as in the north, monthly precipitation sums reach up to 200 mm per month during wet season. In the Ruzizi plain, precipitation sums are much lower, reaching up to monthly sums of 100 mm. This becomes more extreme during dry season, when the monthly precipitation sums in the Ruzizi plain fall down to almost 0 mm. During dry season, most precipitation can be observed at the northern tip of the study area in the region where high mountains are found. This analysis shows that there is a strong difference between the very wet rainy season and the very low precipitation sums during dry season.

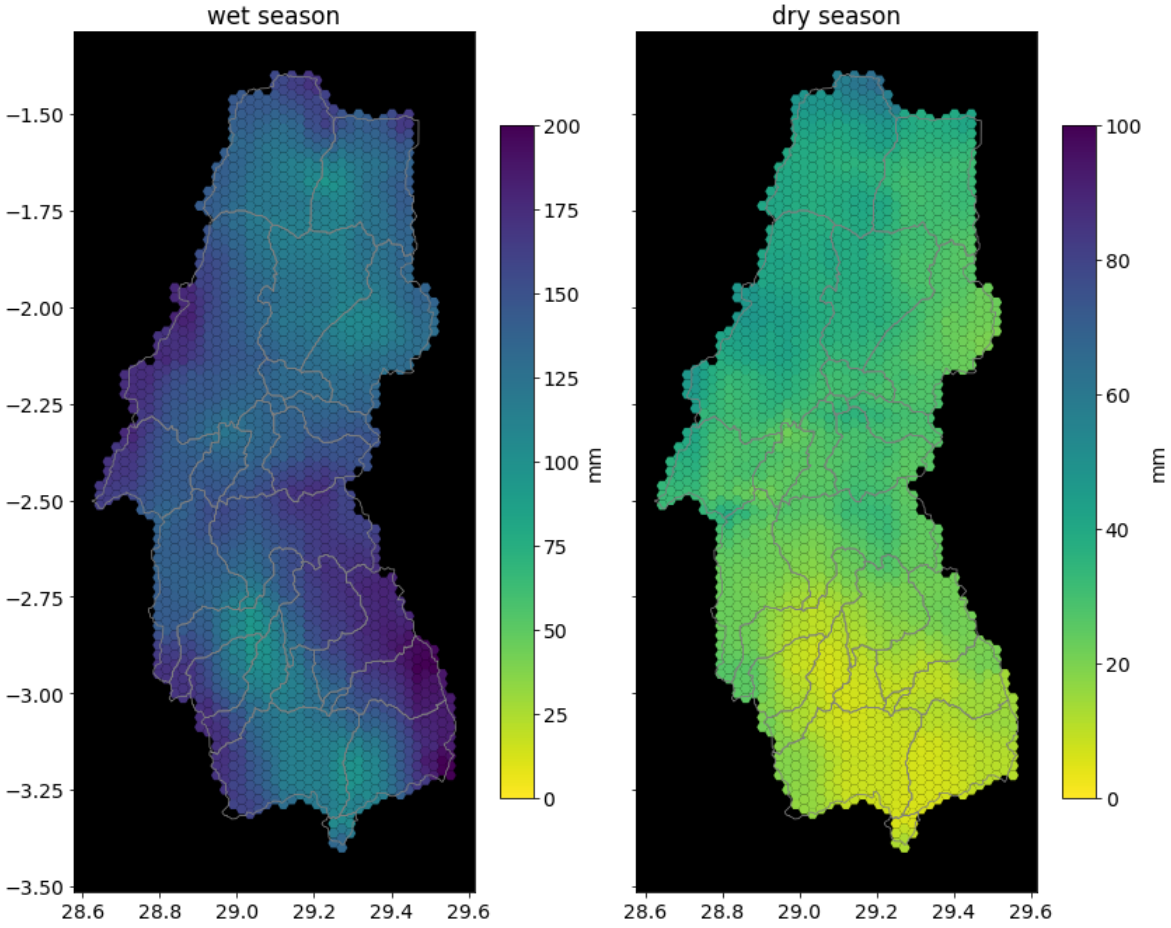

5.1 Mean monthly precipitation sum for months of the dry and wet seasons (2016-2020).

5.3. Extreme Precipitation Events

For the analysis of erosion risk, the monthly precipitation sums only play a subordinate role. It is more important to identify extreme precipitation events that may be short-term and small in spatial extend but are able to wash out sediments due to their high intensity. For this, advantage is taken from the relatively high temporal resolution of the daily data set.

The first step is to determine what daily precipitation sum can be considered an *extreme precipitation* event. For this, it is important to differentiate between wet and dry season. Reason for this is that during wet season, there are likely to be more and stronger precipitation events than during dry season. At the same time, precipitation events during dry season can be able to have a strong effect because soils are dried out and vegetation cover is sparse at this time of the year.

The threshold which determines whether a daily precipitation sum can be considered an extreme event is calculated using each daily data set of the period 2016-2020 on the hexagonal grid. This data is split into dry and wet season data and the 99-percentile is calculated for each hexagon. The 99-percentile gives the threshold precipitation sum for which 99% of the daily precipitation sums are below and 1% is above this value.

The result of this analysis is depicted on figure 5.2. As can be seen from the figure, there are areas in the Ruzizi plain for which a daily precipitation of around 15-20 mm are sufficient to classify this day as an *extreme-precipitation event day* during wet season. At the same time, a daily precipitation of around 50 mm is needed in the mountainous southeastern edge of the study area to classify this day as extreme-precipitation day in the same season. Also for the dry season, the 99-percentile is lowest for the Ruzizi river basin with around 5 mm. Throughout the rest of the study area, the thresholds are distributed without connection to the topography and go up to 25-30 mm.

The 99-percentiles are used to threshold each hexagon of all daily data sets and extract the number of extreme events for each month of the years 2016 to 2020. For the year 2016, figure 5.3 shows the monthly number of extreme events per hexagon. Similar figures for the years 2017-2020 can be found in Appendix A.2.

The distribution of extreme precipitation events in the study area for the year 2016 shows an increased number of precipitation events during March, May and December (wet season) and during August (dry season). The same can be observed from the other years where a larger number of strong precipitation events are found during April/May, August and November/December. The spatial distribution shows a hot-spot of extreme events around lake Kivu in May and in the Ruzizi basin in August 2016 with up to 6 extreme events within a hexagon. Also some stronger events take place during May in the northern volcanic region.

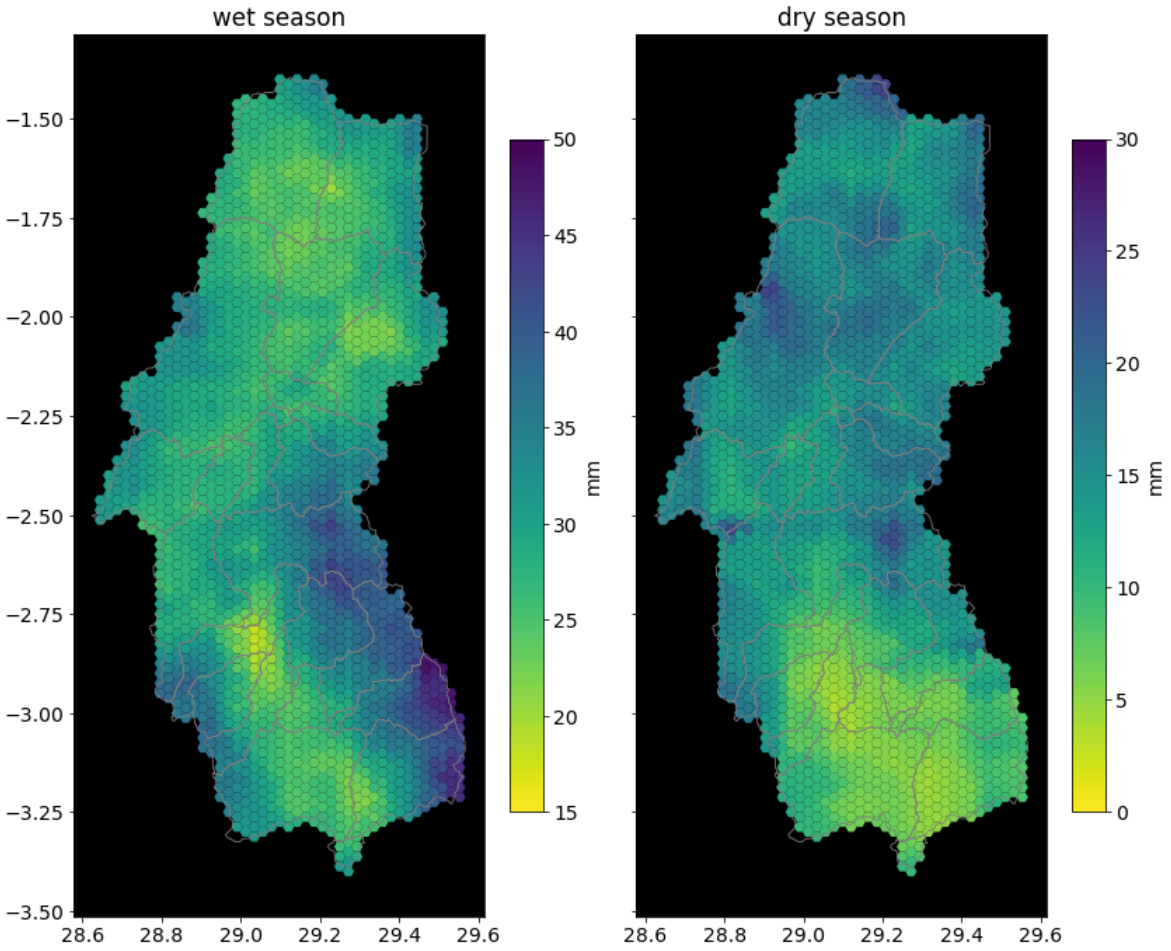

5.2 Value of 99 percentile for each hexagon for wet and dry season derived from all daily data of 2016-2020

6. Erosion Risk Analysis

The previous chapters showed:

1. The analysis of the vegetation dynamics in terms of an NDVI analysis on a hexagonal grid for the years 2016-2020 for both, dry and wet season.
2. The analysis of precipitation events and the identification of extreme events on the same hexagonal grid and for the same period and seasons.

Increased erosion risk is anticipated for those hexagons and periods for which (1) vegetation cover is low and (2) a large number of extreme events is observed. To identify these high risk periods, the results of the vegetation and the precipitation analysis are brought together. This is done by a multiplication of the monthly extreme precipitation events layer with the specific seasonal NDVI. For this, some adaptations to the NDVI layer need to be performed: First, the median NDVI values are normalized to a value range of 0 to 1 and multiplied by -1. A value of 1 is added to the result. Like this, large NDVI values (i.e. dense

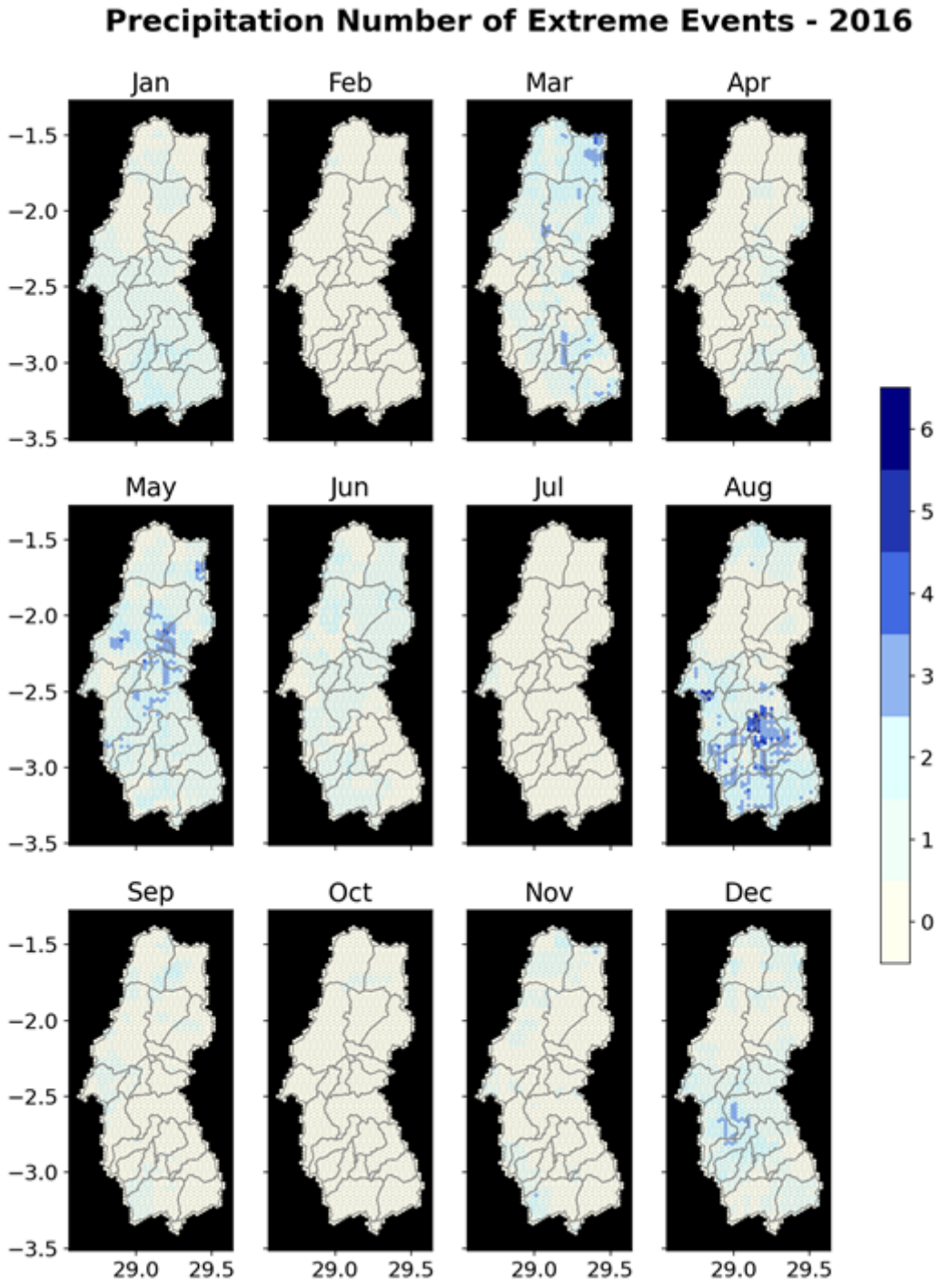

5.3 Mean monthly number of extreme (i.e. above 99-percentile) precipitation events for dry and wet season in 2016.

vegetation cover) get a value close to 0, while low NDVI values (i.e. low vegetation cover or bare soil) have a value closer to 1. This turned-around NDVI range is then multiplied by the extreme-precipitation-events information. In short, the Erosion Risk parameter is

calculated using the following formula:

$$ErosionRisk = ExtremePrecipitationEvents * (normalizedNDVI * (-1) + 1)$$

This results in a monthly erosion risk map which indicates regions of increased erosion risk. Higher values are reached for low vegetation cover and a large number of extreme events. For the year 2016, the erosion risk map is depicted on figure 6.1 while the respective figures for the years 2017 to 2020 can be found in Appendix A.3.

For 2016, the erosion risk analysis shows an extreme erosion risk for the Ruzizi plain during August due to low NDVI values and a large number of extreme precipitation events. Also in June an increased erosion risk throughout most parts of the study area is found. During wet season, the months January, March, May and December show an increased risk. However, values as high as for August and for such a large area are not found throughout the rest of the year. Along the forested mountain ridge in the southeast, a very low to low erosion risk is calculated for each month due to the high year-round NDVI found here. For the year 2019, the most abundant high erosion risk can be found in May which covers almost the entire study area. In November, high risk can be found along the northern and eastern coast of lake Kivu. In contrast to the year 2016, the erosion risk hot-spots are located around the lake rather than in the Ruzizi basin. Another hot-spot for extreme erosion risks is found for June 2019 with very high values for the Ruzizi plain and the southern edge of lake Kivu.

The results show that there is not one single hot-spot region for which and increased erosion risk is predicted. The distribution of increased erosion risk is strongly dependent on the distribution of precipitation events which varies from month to month and from year to year. Furthermore, the seasonal NDVI and the distribution and intensity of low vegetation cover varies for each year. However, there seem to be two main areas with increased erosion risks, i.e. the Ruzizi plain and the northern and eastern area around lake Kivu. This will be further discussed in chapter 8.

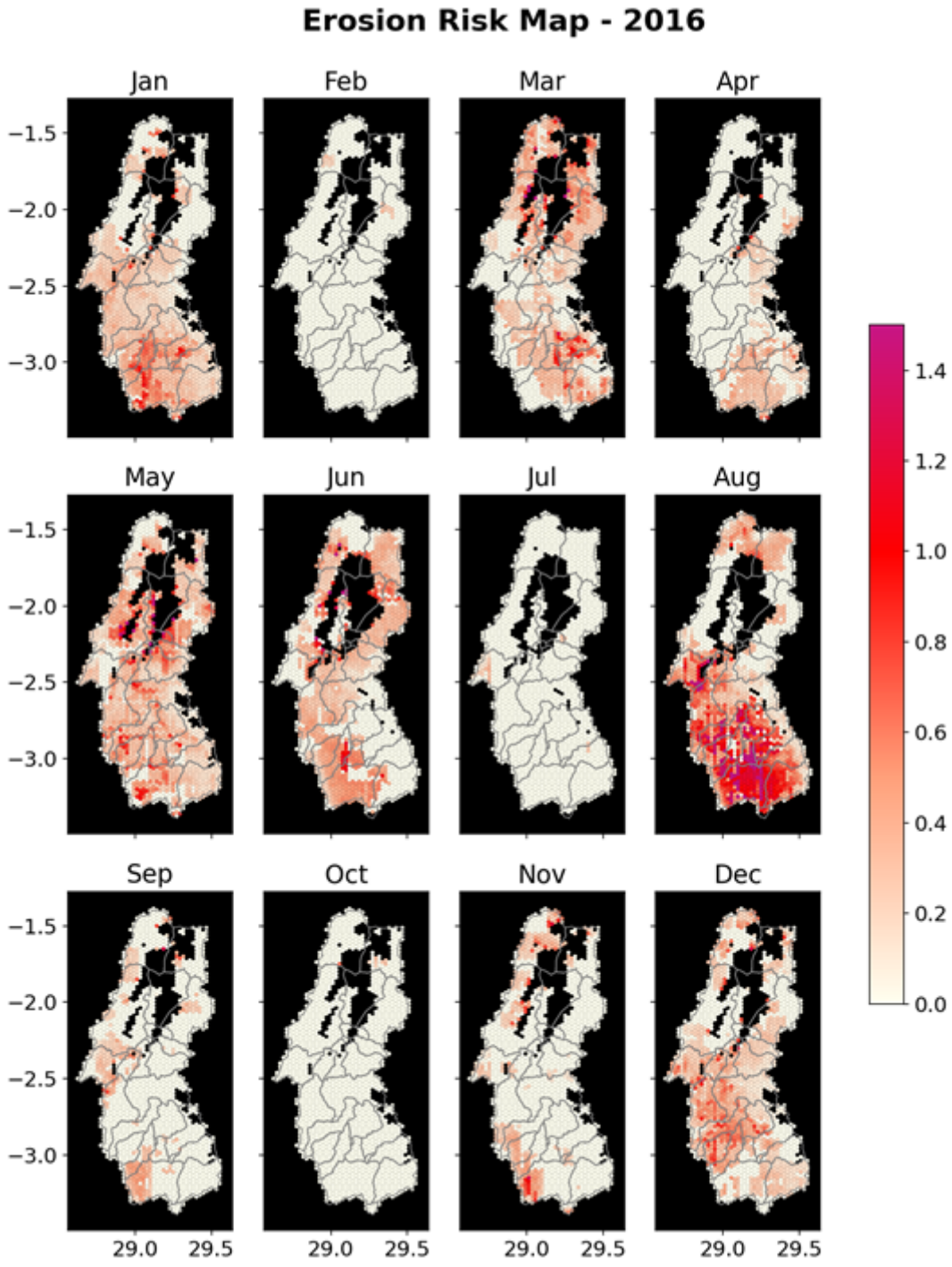

6.1 Erosion risk map derived from the multiplication of NDVI and precipitation for dry and wet season of 2016.

7. Work Package 3: Turbidity Analysis Lake Kivu

In this chapter, the turbidity of lake Kivu is analyzed. The goal of the analysis is to test whether turbidity can be used as indicator for previous soil erosion. Like this, the turbidity data can be connected to the erosion risk analysis of the previous chapter. The hypothesis is: When there is increased erosion risk, the turbidity of the lake is increased due to increased sediment intake into the lake.

7.1. Data

For the turbidity analysis, the EO-based turbidity product of the Copernicus Global Land Service (CGLS, `https://land.copernicus.eu/global/products/lwq`) is used. It is available for May 2002 - March 2012 and from May 2016 to today. In the earlier period, the data set is based on data from the ENVISAT-MERIS sensor, while the latter period is based on data of Sentinel-3. Since the second period from 2016 fits well to the period considered in this study, the analysis focuses on the Sentinel-3 based product. There is one data product every 10 days in a resolution of 300m. The data is aggregated to monthly means for the analysis.

7.2. Seasonal Turbidity

Figure 7.1 shows the monthly mean turbidity based on the CGLS turbidity data set for the year 2017. As can be noted from the figure, an increased turbiditiy often occurs at the coast of the lake. One reason for this can be sediment inflow through rivers. Other causes of this increase can be the disturbance of the lake ground in shallow waters due to waves, water inflow or human activity. The annual cycle of the turbidity in the lake shows a tendency of increased turbidity during wet seasons. Especially in March, April and from October to December, the data shows increased turbidity with a peak in November. During dry Season, i.e. in July, August and September, water turbidity is lower than throughout the rest of the year. This annual cycle is also visible in other years (see figures in the appendix: 1.13, 1.14, 1.15 and 1.16) with a minimum lake turbidity in August and increased turbidity in March/April and from October to December.

On figure 7.2, a comparison is shown between the erosion risk (left side of the panel) and the turbidity (right side) for May 2017. In May 2017, a very high erosion risk is detected for the area around lake Kivu. Especially in the southwestern lake but also on the eastern and northeastern coast, the erosion risk peaks. The turbidity on the right clearly shows increased values along most of the coastline. Especially in river deltas, an increased turbidity can be noted. This can be a sign, that increased soil erosion might have taken place in May 2017.

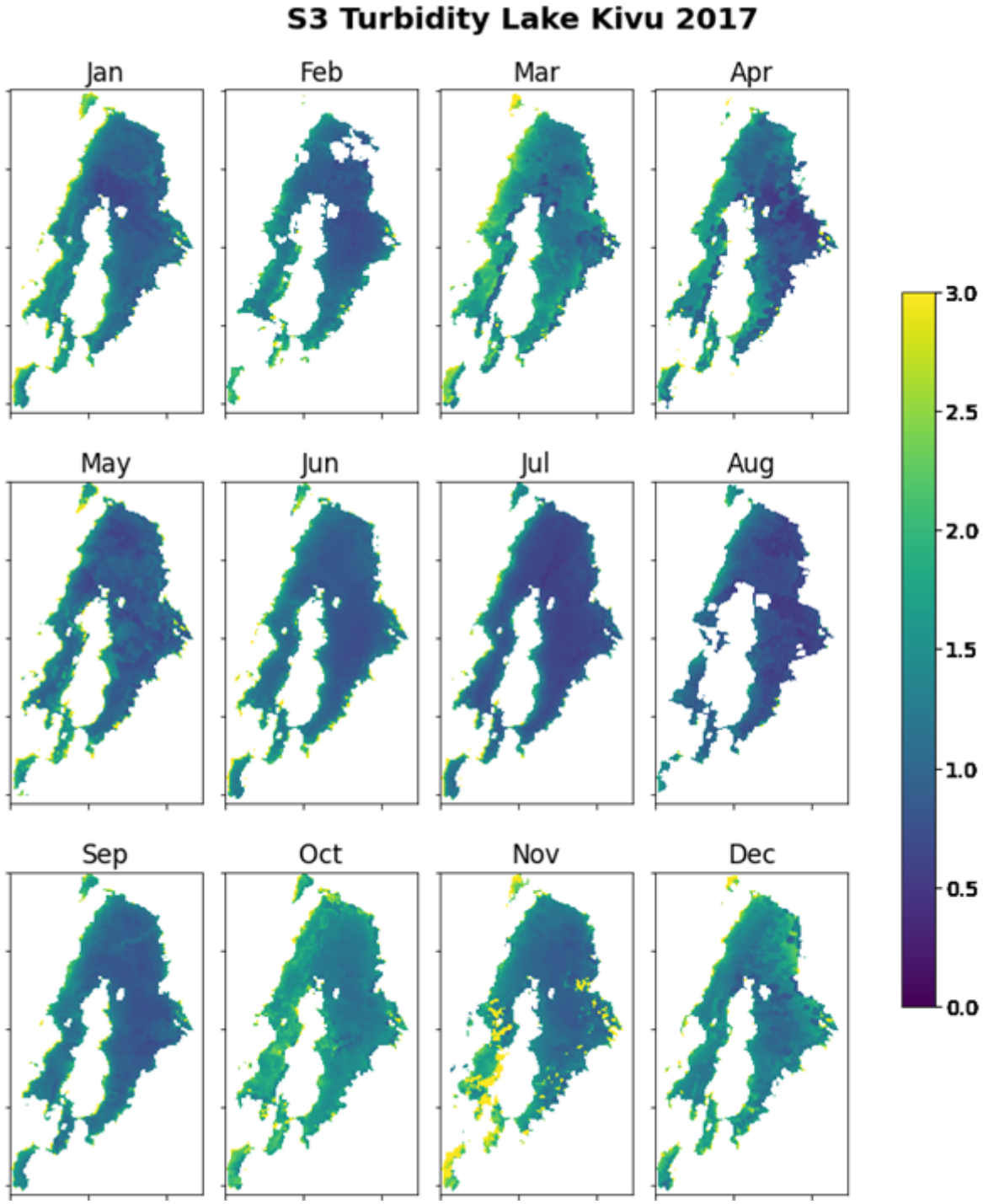

7.1 Monthly mean turbidity for 2017 of lake Kivu based on the CGLS Sentinel-3 turbidity data.

To identify the connection between lake turbidity and erosion, a second more quantitative analysis is performed. For this, the sub-basins around lake Kivu are subdivided according to the part of the lake, in which their main flows terminate. Like this, each sub-basin is assigned to northern, eastern, southern and western basins. This is illustrated on figure

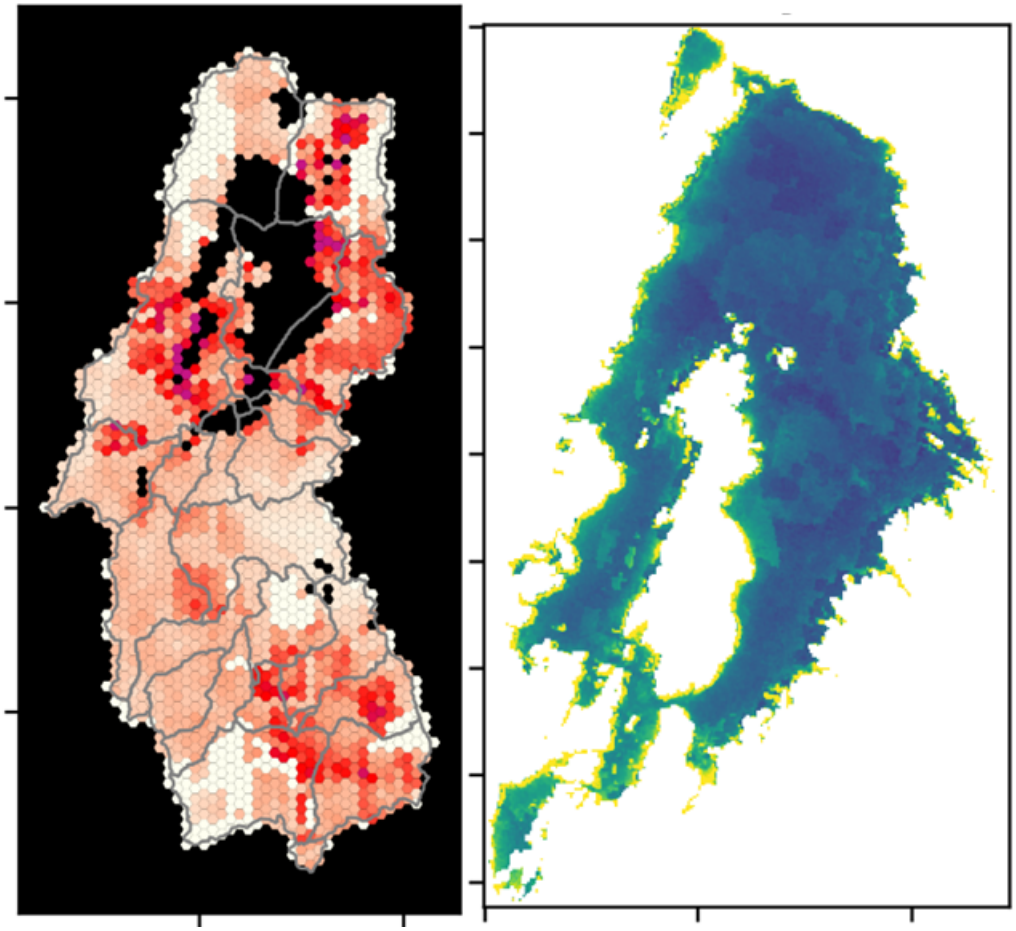

7.2 Comparison of erosion risk (left) and turbidity (right) for May 2017.

7.3. The monthly erosion risk of each basin is calculated using the mean of each hexagon within each basin. This is compared to the monthly mean lake turbidity within the first kilometer of the lake from the coast, indicated by the red line within the lake area on figure 7.3 (left). The right side of the same figure shows the correlation between mean erosion risk of the basins and the mean turbidity.

As can be noted from the scatterplots on the right panel of figure 7.3, there is no clear connection between the two parameters. However, for most zones, except zone *North*, there are only few months with high erosion risk and low lake turbidity.

Overall, it can be concluded that the CGLS Sentinel-3 lake turbidity product has a suitable coverage and resolution to detect changes in the lake turbidity. In this project, it could be used to identify seasonal changes. However, it is difficult to draw a connection between erosion risk and lake turbidity. Reasons for this may be:

1. Although an increased erosion risk has been identified for the region, it is not clear if erosion really took place.
2. The averaging of the turbidity to monthly scales is likely to lead to a dilution of the sediment inflow events as they may be short in time. The same is true for the spatial

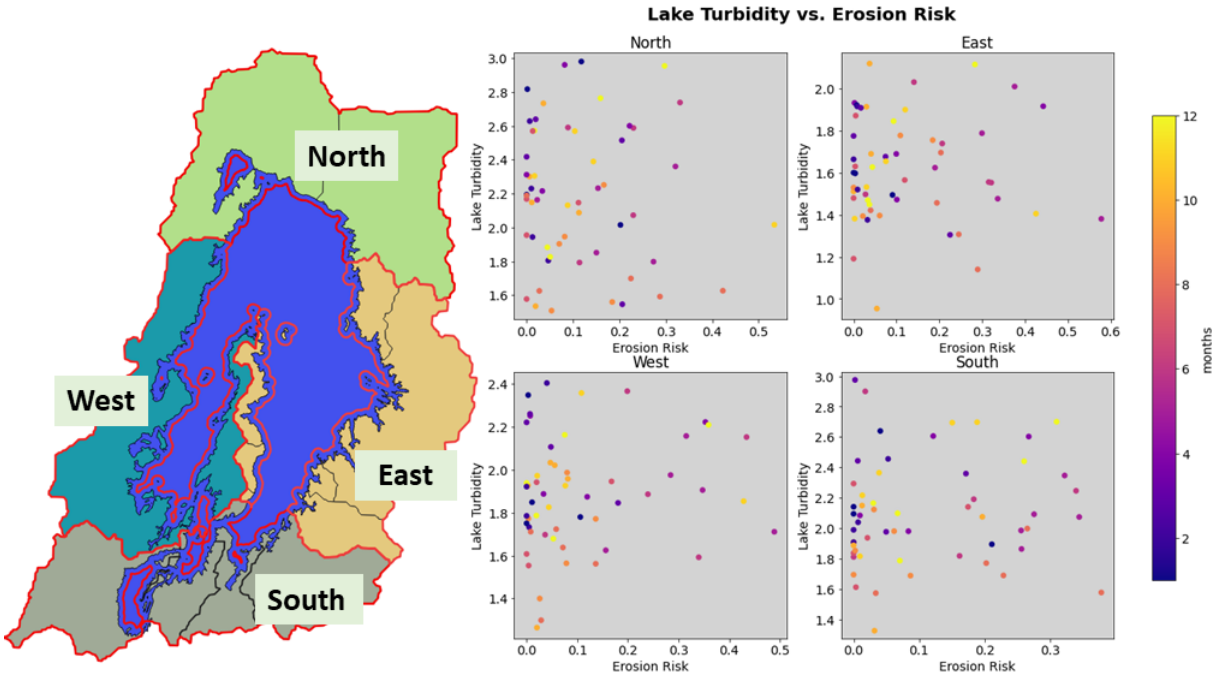

7.3 Subdivision of catchment areas around lake Kivu into North, East, South and West (left) and scatter plot of lake turbidity vs. erosion risk for each month from 2016 to 2020.

aggregation as river inflows are small in size.

3. The turbidity can be influenced by a number of different factors that are independent from erosion. This includes wind, waves or human activity.

The generalization of the data in space and time was inevitable due to the large scale of the lake and the intention to perform the analysis in an automated way for the whole area. Furthermore, the data availability of the product does not allow for the analysis of shorter time steps. In future analyses, a more detailed look should be taken into small scale river inflows. Like this, it is likely that the turbidity data can be a real asset to identify and validate erosion events.

8. Comparison of the Erosion Risk Map and the RUSLE simulations

To make the Erosion Risk Map comparable to the results of the RUSLE simulations performed in the *Baseline Study for the Basin of Lake Kivu and Ruizizi River* (*Sher Consult*, 2020), a five-year mean is calculated from the results of chapter 6. For this the sum over each month in the five years from 2016 to 2020 is calculated and divided by five. The result is shown on figure 8.1B). On this map, the main hot-spots over the full time period can be identified and compared to the RUSLE results depicted on figure 8.1A). The erosion risk hot-spots of the EO analysis are located

1. at the Ruzizi plain: This is due to the agricultural land use and the regular harvesting and plowing of the agricultural fields found in this area. Furthermore, very low precipitation occurs in this area during dry season, which leads to further drying off of the vegetation in the river plain.
2. at the area north of lake Kivu between the city of Goma and the volcanic area. The area is covered by cropland, which again leads to regular open soil periods and may cause soil degradation.
3. at the city agglomerations of Goma and Bukavu. For this area, low vegetation cover is detected which leads to an increased erosion risk. The low vegetation cover is probably a result of the cities themselves, the city growths, the infrastructure and other human activities, e.g. small scale agriculture.
4. east of lake Kivu, where a lot of grassland is found and vegetation cover strongly declines during dry season.

It stands out that the erosion risk is very low in the area of Nyungwe Forest and Kibira National Park. Due to the forest cover, high NDVI values are found throughout the year. This leads to a low erosion risk although the mountainous region experiences some strong precipitation events. This shows how important it is for soil conservation to keep these ecosystems in a healthy state and to keep areas covered by vegetation throughout the year, especially in humid environments.

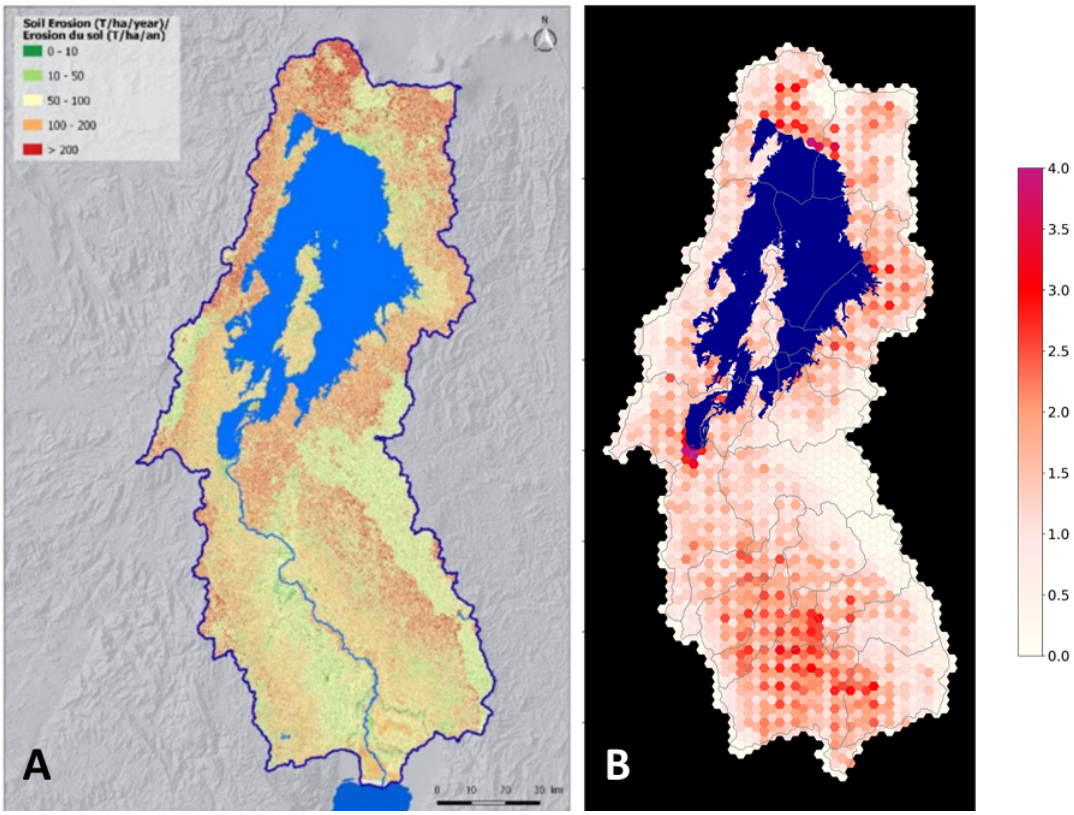

8.1 A) Soil erosion in T/ha/year derived from the RUSLE model simulations performed and described in (Sher Consult, 2020). B)5-year-mean annual sum of erosion risk derived from the EO analysis.

The RUSLE model comes to a similar result like the EO analysis: The main hot spots are located in the Ruzizi plain (although a bit further east than in the EO analysis), north of lake Kivu in the volcanic area and along the eastern and western coast of the lake. Very low erosion is predicted for the southeastern mountain range where the conservation areas are located.

9. Work Package 4: Urban Growth Simulation for the Cities of Goma and Bukavu

9.0.1. Introduction SLEUTH Model

SLEUTH is an acronym for slope, land use, exclusion, urban extent, transportation and hill shade, which are the input data required by this model. It is a cellular automaton (CA) model of urban growth and land use change. The model is based on the "Clark Cellular Automaton Urban Growth Model" published by *Clarke et al.* (1997). It consists of two coupled cellular automata models: one for urban growth modelling (UGM) and the other for land use change (LUC) prediction. In this application, the UGM was applied to the study areas. The basic assumption of the model is that every city has its own "DNA". This "DNA" is controlling the growth process of the city. Without any influence from outside, the city will always grow according to its "DNA" as it grew in the history. To describe the urban growth process, four growth behaviors are defined:

- Spontaneous growth: this growth is described as occurrence of a random distributed pixel that is urbanized.
- Diffusive growth: defines if a newly urbanized pixel will become a new spreading center.
- Organic growth: this behavior defines urbanization happening along the edges of a spreading center.
- Road influenced growth: defines urban growth along the road network.

These four behaviors are based on the cell-based structure of an image, also known as pixel based. They are quantified and controlled by five different coefficients:

- Diffusion: it defines the dispersiveness of the distribution of grid cells and the movement of new settlements outward from the road network.
- Bread: it defines the likelihood that a new settlement is being generated.
- Spread: it controls how far outward organic expansion takes place.
- Slope resistance: it represents a resistance to steep slope.
- Road gravity: it defines the ability of attracting new urban pixels close to the existing road system.

The "DNA" of a city lies in these five coefficients as they control the behaviors of the city growth directly or indirectly. To derive a set of optimal combination of coefficients that can simulate the historical urban growth of the city, a calibration phase is applied. Traditional SLEUTH calibration contains three steps: coarse calibration, fine calibration

and final calibration. These three steps are defined by different scales of their inputs and are known as “brute-force calibration” (*Clarke et al.*, 1997). This calibration strategy was later replaced by a genetic algorithm (*Clarke*, 2017). Coefficients generated from calibration will be used to simulate the future urban growth of the city. In this study, the genetic algorithm-based SLEUTH (SLEUTHGA) was implemented.

9.1. Study areas

The SLEUTH model was applied to two city agglomerations: the Goma city agglomeration and the Bukavu city agglomeration. The Goma city agglomeration is a region that spans between latitudes 1°35´ - 1°42´S and longitude 29°60´ - 29°20´E. It covers the city of Goma and also includes cities near to it in the Democratic Republic of Congo (DRC) and the Republic of Rwanda (Rwanda). The Bukavu city agglomeration lies between latitudes 2°27´ - 2°35´S and longitude 28°47´ - 28°56´E. It covers the major city of Bukavu and cities in DRC and Rwanda. Both city agglomerations are on the side of Lake Kivu and are the two biggest city agglomerations around the lake.

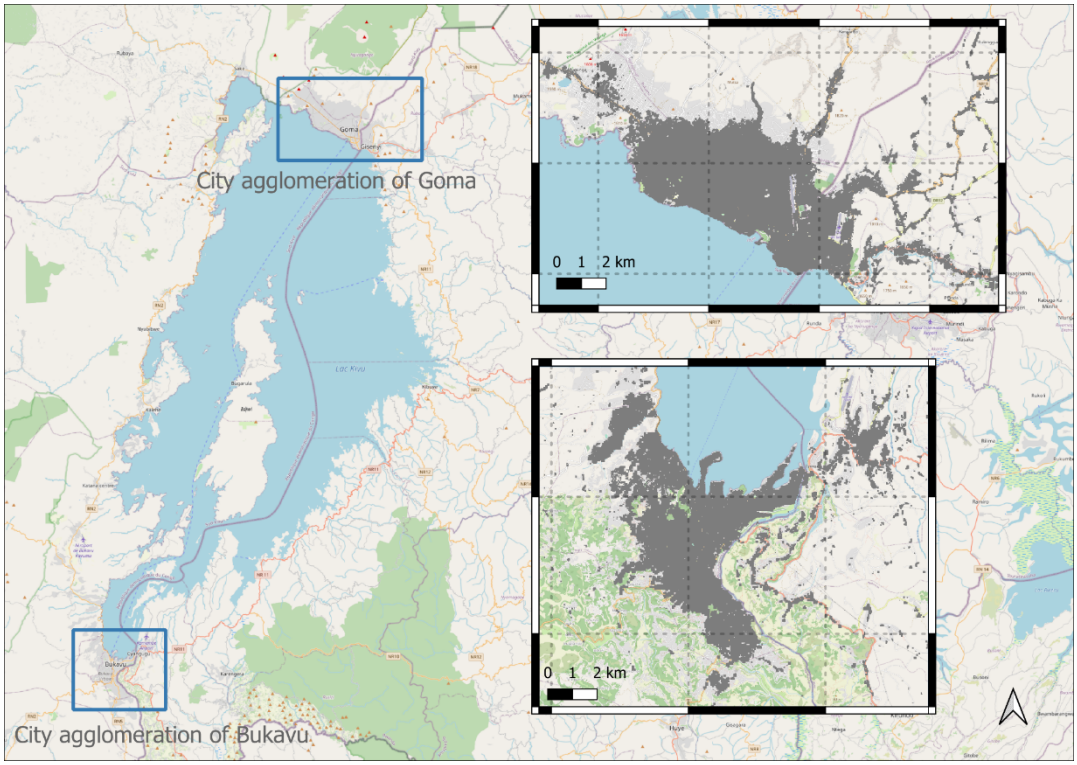

9.1 Outlines of areas for which SLEUTH simulations are performed.

9.2. Data

SLEUTH contains two models and requires 6 types of input to simulate the urban growth in the future. For the UGM, 5 inputs are sufficient. These are: slope, excluded areas layer,

urban layers, traffic layers and hill shade layer. In order to better simulate the growth of a city, the history behind it should be taken into consideration. Both DRC and Rwanda suffered from civil wars starting in the 1990s for different periods. To better consider the local historical events that cause effects on historical urban growth in the corresponding regions, each of the two city agglomerations were separated into two parts along their national boundaries. Traditional brute-force calibration requires at least 4 historical urban layers. For GA based SLEUTH model, this is no longer mandatory. The urban layer from the earliest year will be automatically defined as seed layer, meaning that all future urban growth will happen based on the extent of the city in this year. The rest of the urban layers will be used as reference layers to control the simulation of urban growth. The World Settlement Footprint (WSF) (*Marconcini et al.*, 2020) is a global time series data of urban extent that has a temporal resolution of one year, ranging from 1985 to 2015. The urban layers that are used in this study were generated from the WSF. Considering the war period of both countries, we utilized only historical urban layers after 2000. In this study, the layers of 2000, 2002, 2005, 2008 and 2010 were used for calibration and the urban layer of 2015 was used as a reference for evaluation.

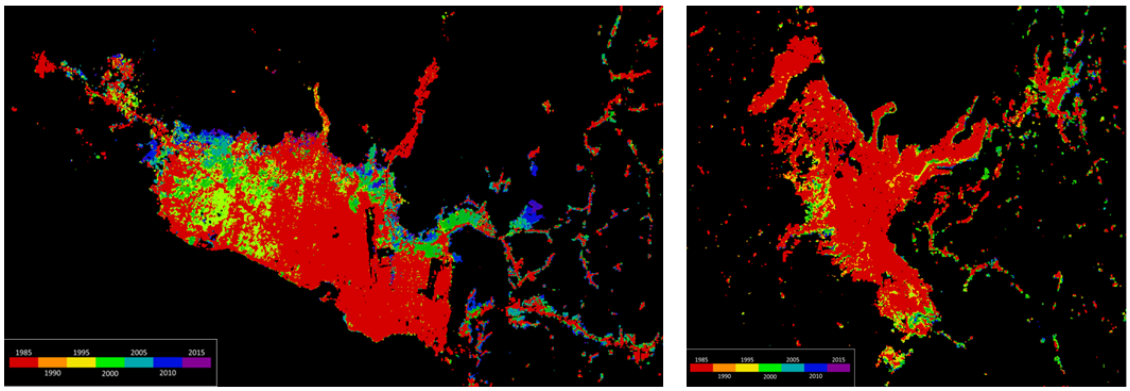

9.2 Color-coded WSF of two study areas

Excluded areas indicate where the city cannot grow in the future e.g. water, natural preserved areas, industrial used land or military used land. In this study, water and natural preserved areas were taken into consideration. The water mask layers for both regions were generated from Sentinel-1 satellite images. The natural preserved areas layers were obtained from the World Database on Protected Areas (WDPA) and other effective area-based conservation measurement (OECM) (`https://www.protectedplanet.net/`). These two layers were combined into one binary excluded areas layer and served as input for the SLEUTH model. The traffic layer gives information on the location of the road network, which is essential for calculating the road gravity coefficient. The SLEUTH model requires at least two road layers from different epochs for the calibration. In this study the road layers were obtained from The Global Road Inventory Project (GRIP) database (`https://www.globio.info/download-grip-dataset`). The Slope and hill shade layers were generated from a digital elevation model (DEM). In this study, Copernicus DEM at 30 meters resolution (`https://panda.copernicus.eu/`) was used.

9.3. Results and Discussion

As mentioned in 2.2, both city agglomerations were separated into two parts according to the national boundaries. In total, 4 SLEUTH models were calibrated with respect to their regions. The optimal SLEUTH Metric (OSM) (*Dietzel and Clarke*, 2007) and a Receiver Operating Characteristic (ROC) curve were employed for the evaluation. Based on the ROC curve, the Area Under the Curve (AUC) was calculated. An AUC larger than 0.75 means the corresponding model has a good ability for prediction. After evaluation, a future prediction of the urban growth up to 2050 was implemented based on a seed urban layer of 2015.

9.3.1. City agglomeration of Goma in DRC

The City-agglomeration of Goma on the DRC side includes the city of Goma, Nyiragongo, MasisiIdjwi, and Kalehehas. It covers an urban area of 50.4135 km2 (based on resolution of 30m) in 2015. The evaluation of the simulation results gave an OSM of 70.16% and an AUC value of 95.99%, which shows that SLEUTH has been well calibrated in this region. After the calibration, a prediction to 2050 was applied to this region. The SLEUTH model produces a probability map for the predicted urban extent, giving an urbanization probability value for each pixel. To better represent and analyze the future urban extent, a probability threshold of 80% was selected based on the assumption that pixels with a probability larger than 80% will be defined as urban pixels in the year 2050.

Results show a growth along the northern part of the city due to the flattened terrain in this region. The northwestern part seems to have more growth than the western part. Overall, the city would expand itself by 7.6887 km2.

9.3.2. City agglomeration of Goma in Rwanda

The city-agglomeration of Goma on the Rwanda side includes the city of Gisenyi, Cyanzarwe, Busasamana, Nyundo, Nyamyumba, Nyakiriba, Lac Kivu and Rugerero. It covers an urban area of 20.403 km2 in 2015. Evaluation of the SLEUTH model output for this region returned an OSM of 45.41% and an AUC of 92.39%.

The prediction to 2050 shows a rapid urban development in this region: according to the model the city will double in size and expand by 26.1888 km2. Most of the newly developed city clusters will happen along existing city clusters and the proportion of such a growth near a road would be higher than the growth near the original city agglomeration on the western side.

9.3.3. City agglomeration of Bukavu in DRC

The city agglomeration of Bukavu in DRC is located south of lake Kivu. This region overs the city of Bukavu, Kabare, Walungu, and possesses urban areas of 33.4521 km2 in 2015. The results of the calibration show a strong slope resistance in this region, due to its complicated terrain. The evaluation based on the map of 2015 returnes an OSM of 84.82%

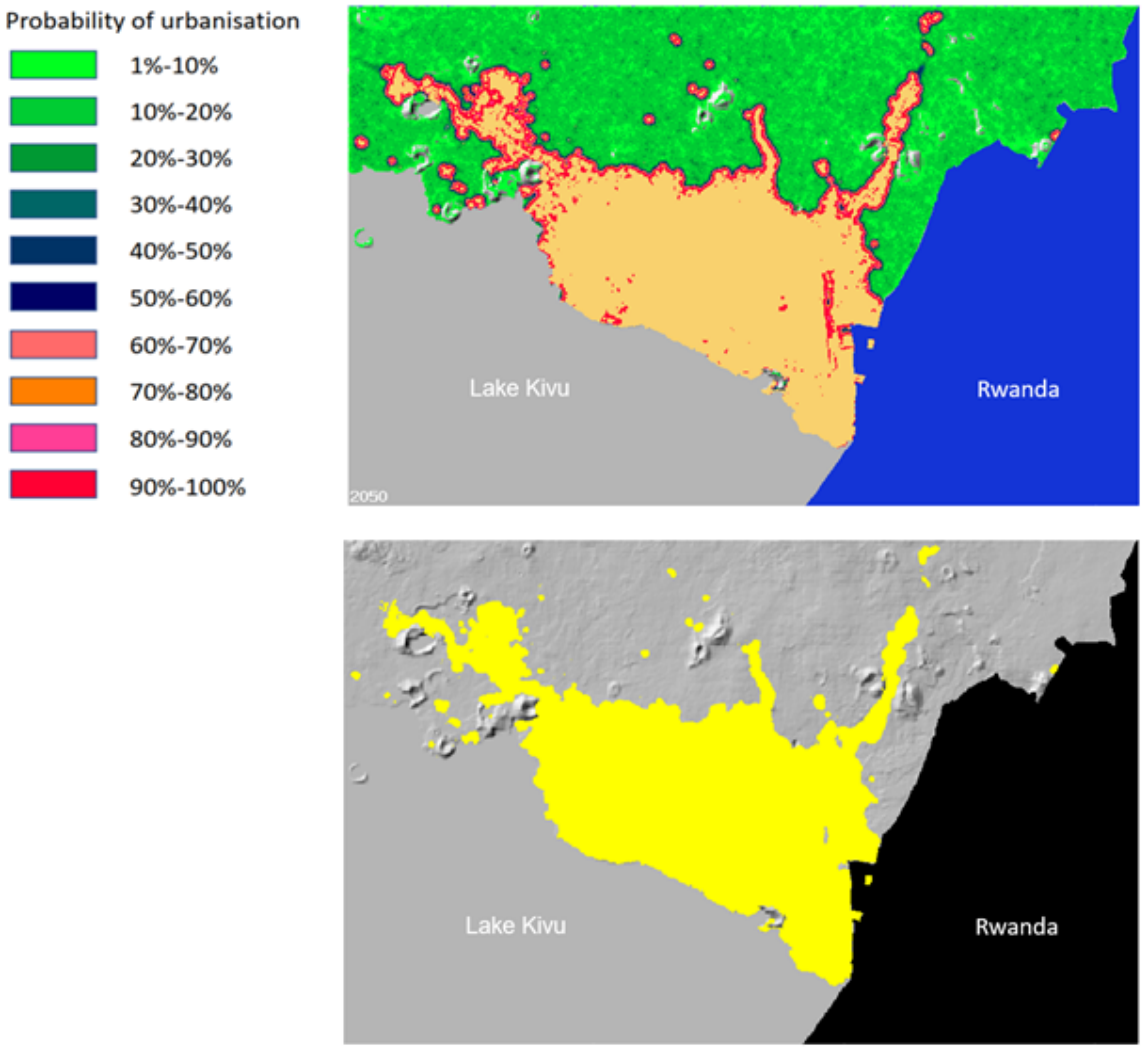

9.3 Predicted probability map and predicted urban extent map of Goma city agglomeration in DRC

and an AUC of 88.73%.

Unlike the region of Goma, this region is surrounded by a mountain range. Since the presetting of the SLEUTH defines a slope threshold of 21 degrees, the model does not simulate city growth on any slope that is steeper than this threshold. Therefore, the predicted probability map of 2050 demonstrates a slow development in the future. However, according to the model, there will still be some minor urban developments happening on flattened areas like coastal regions. In total, there will be 1.3878 km2 urban areas that develop up to 2050.

9.3.4. City agglomeration of Bukavu in the Republic of Rwanda

The city agglomeration on the Rwandan side distributes itself in a scattered way. It contains the major city of Gihundwe, as well as parts of cities of Gashonga, Giheke, Kamembe, MururuLac and Nyakarenzo. The biggest city cluster in this region is the Gihundwe, in

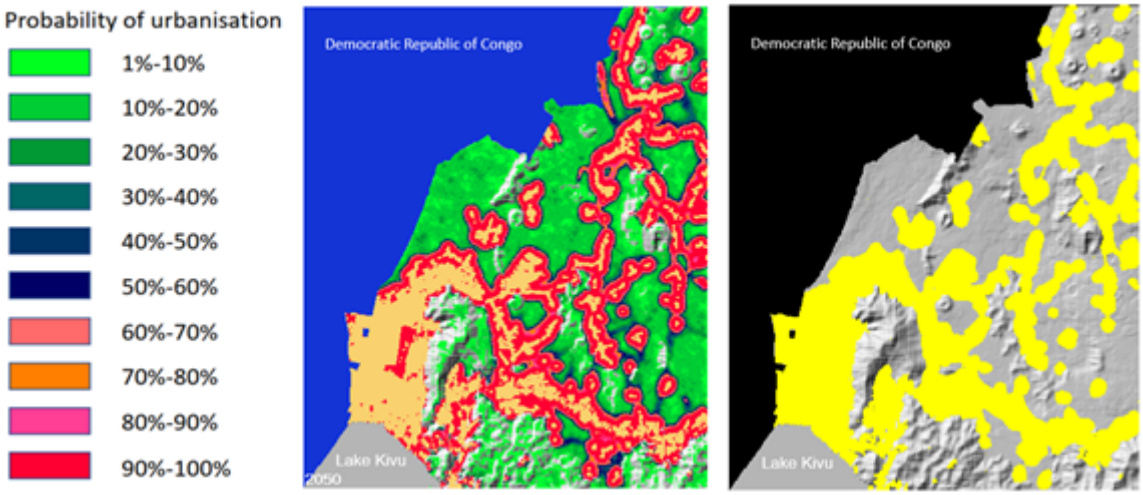

9.4 Predicted probability map and predicted urban extent map of Goma city agglomeration in Rwanda

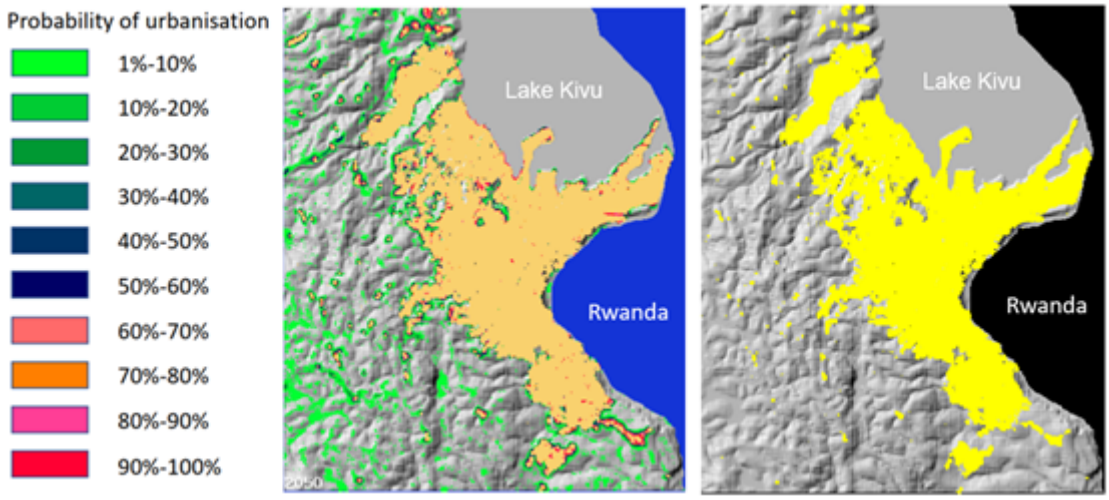

9.5 Predicted probability map and predicted urban extent map of Bukavu city agglomeration in DRC

total, this region contains city areas of 7.8552 km2 in 2015. The evaluation of the model returned an OSM of 74.84% and an AUC of 82.45%.

The predicted probability map shows no growth in this region, although some areas would have potential to be urbanized in the future, the probability of this growth is mostly lower than 20%. The first reason for it is because of an extreme low growing ratio in this region between 2000 to 2010. Since SLEUTH is learning from historical growth, the predicted growing process will also be slow in the future. Another factor to be considered is the terrain in this region. Due to a strong slope resistance coefficient, the city growth is limited on steep slope. Hence, according to the prediction, the city will not change significantly until 2050.

The distribution of predicted urban growth to 2050 of two city-agglomerations is shown in Fig. 9.7.

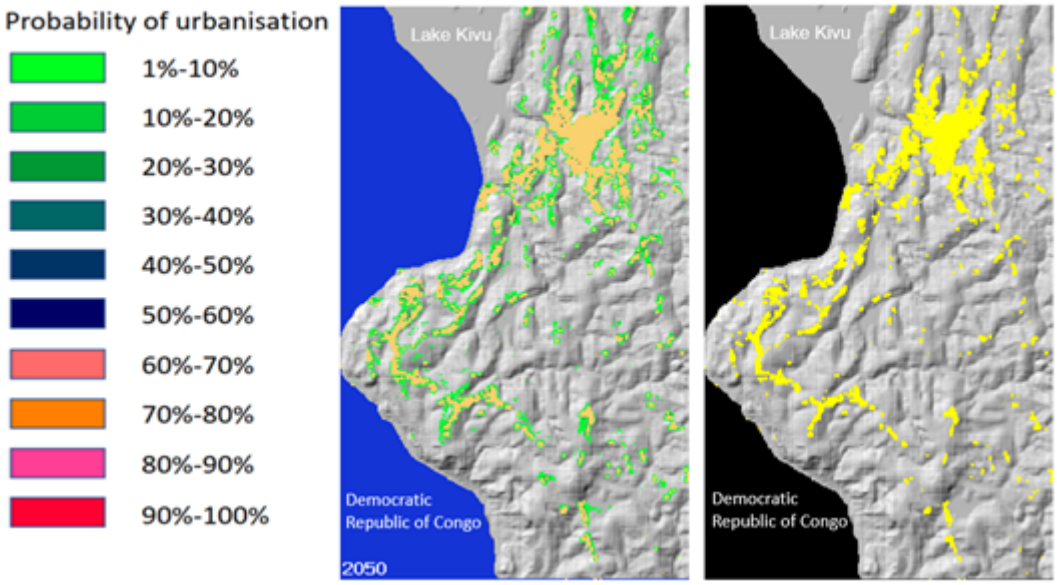

9.6 Predicted probability map and predicted urban extent map of Bukavu city agglomeration in Rwanda

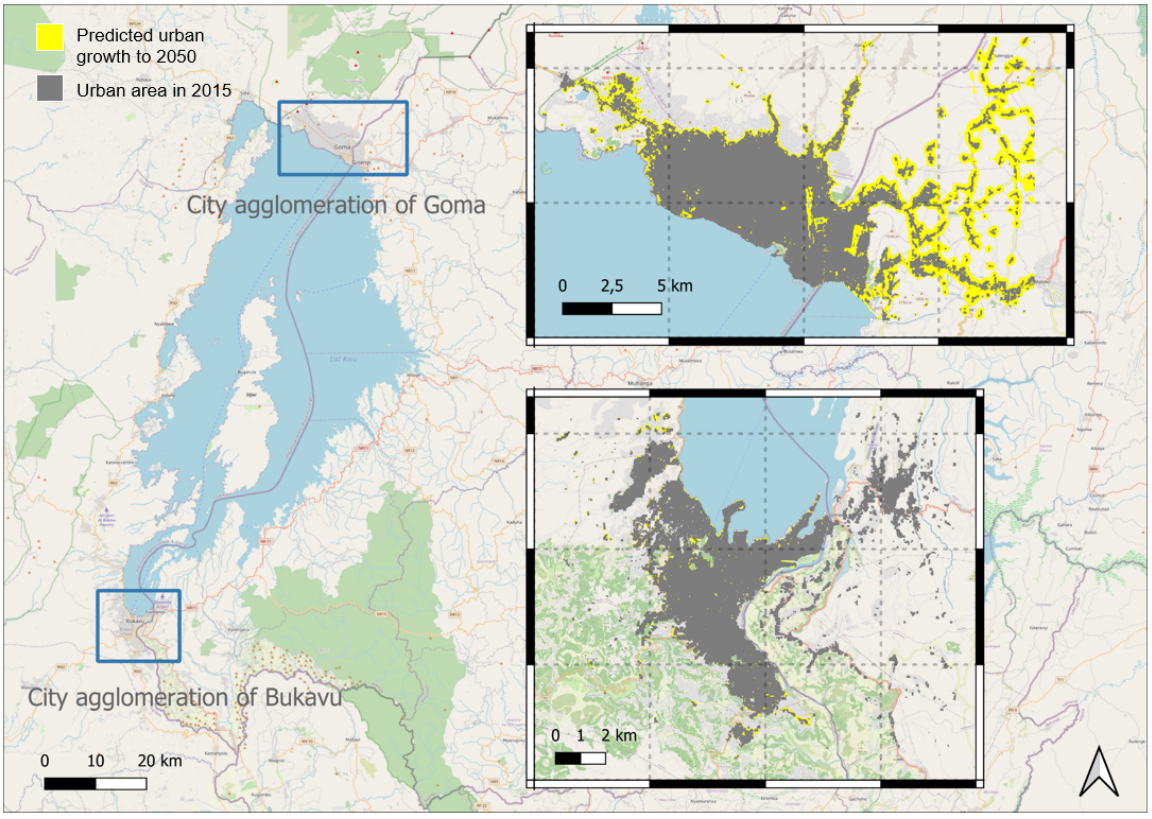

9.7 Predicted urban growth to 2050.

A. Appendix

A.1. Work Package 1: Vegetation Dynamics

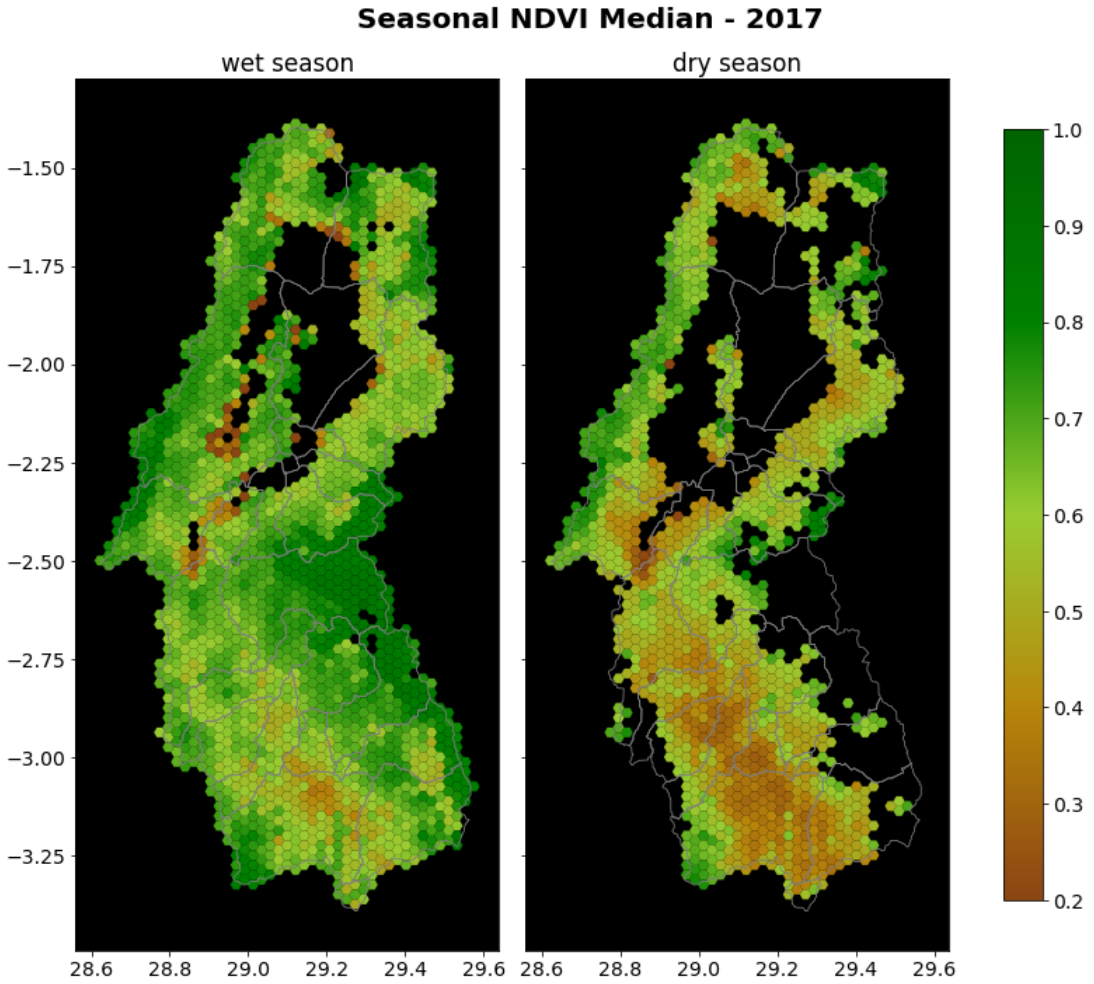

1.1 NDVI median of 2017 for the dry and wet season.

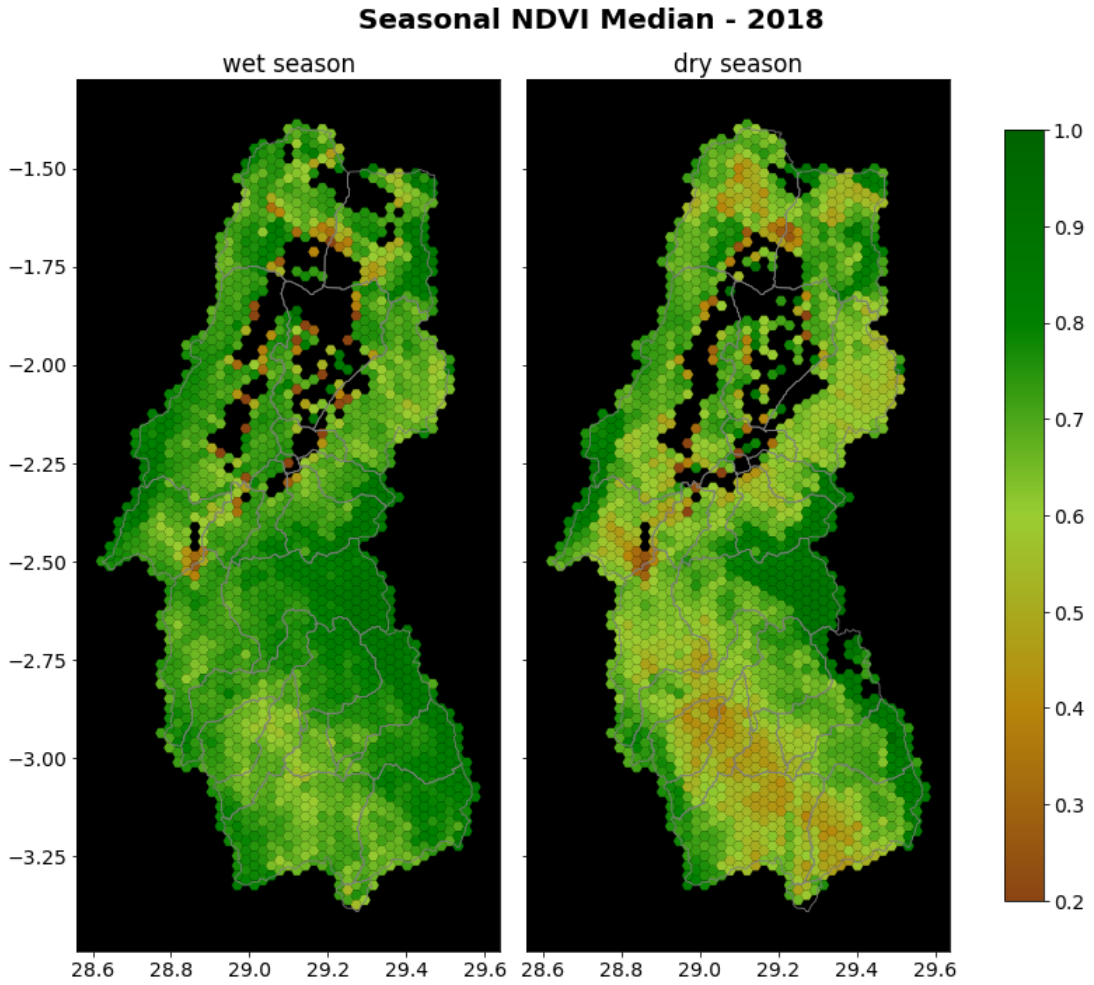

1.2 NDVI median of 2018 for the dry and wet season.

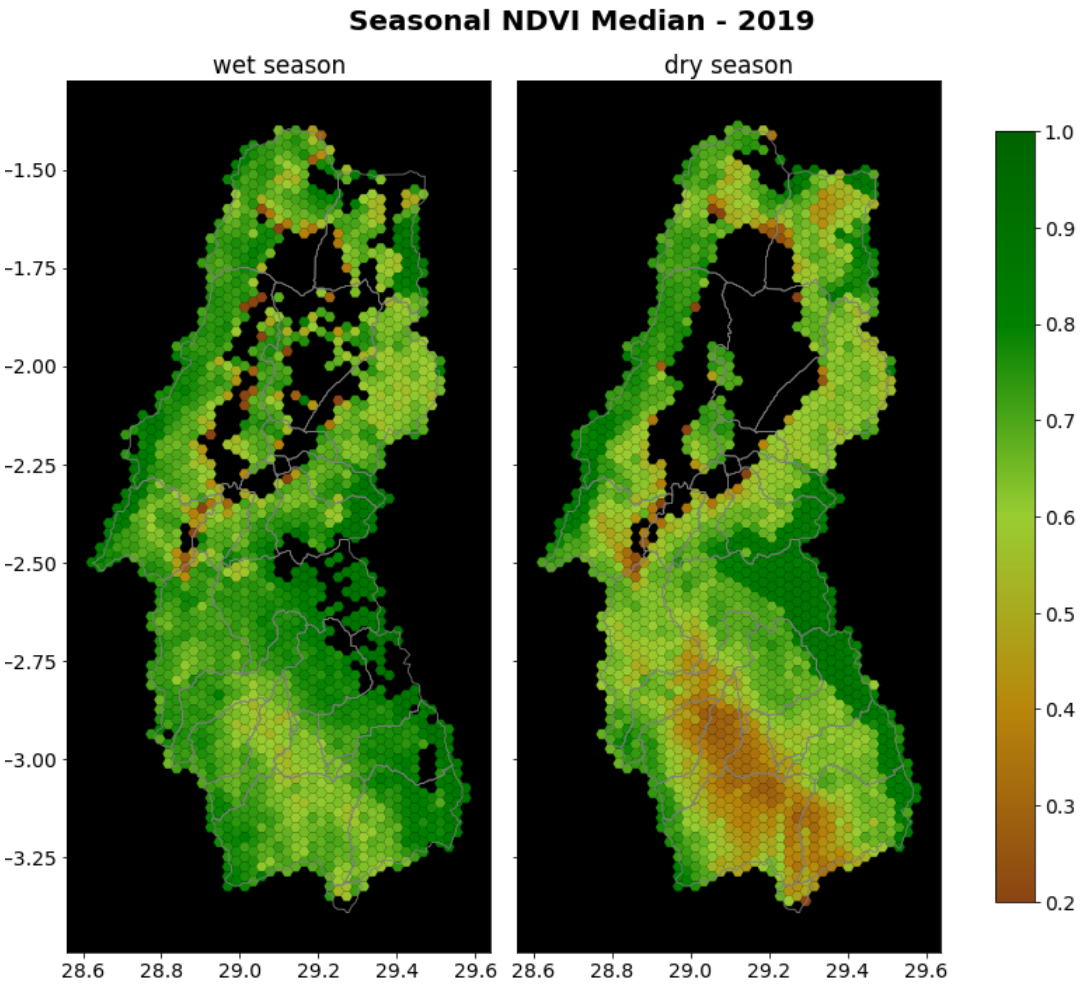

1.3 NDVI median of 2019 for the dry and wet season.

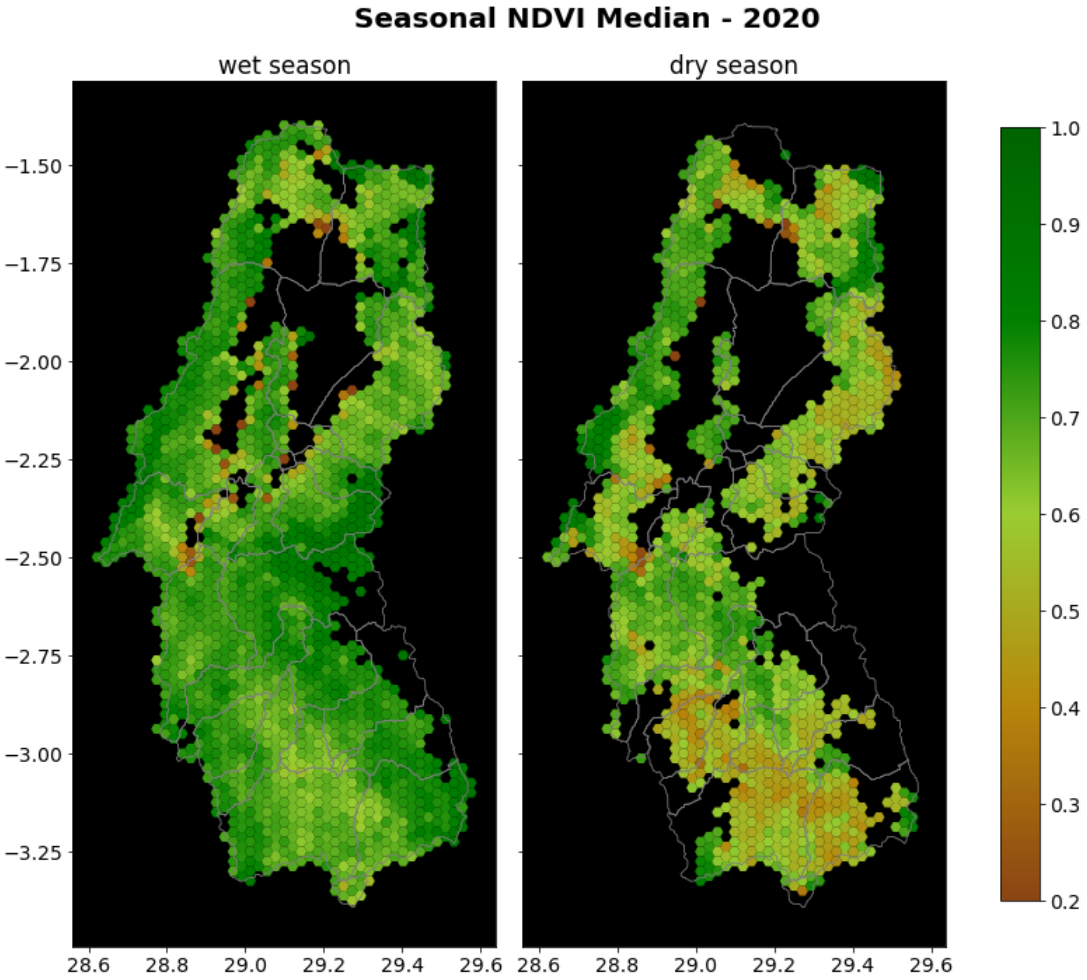

1.4 NDVI median of 2020 for the dry and wet season.

A.2. Work Package 2: Precipitation Analysis

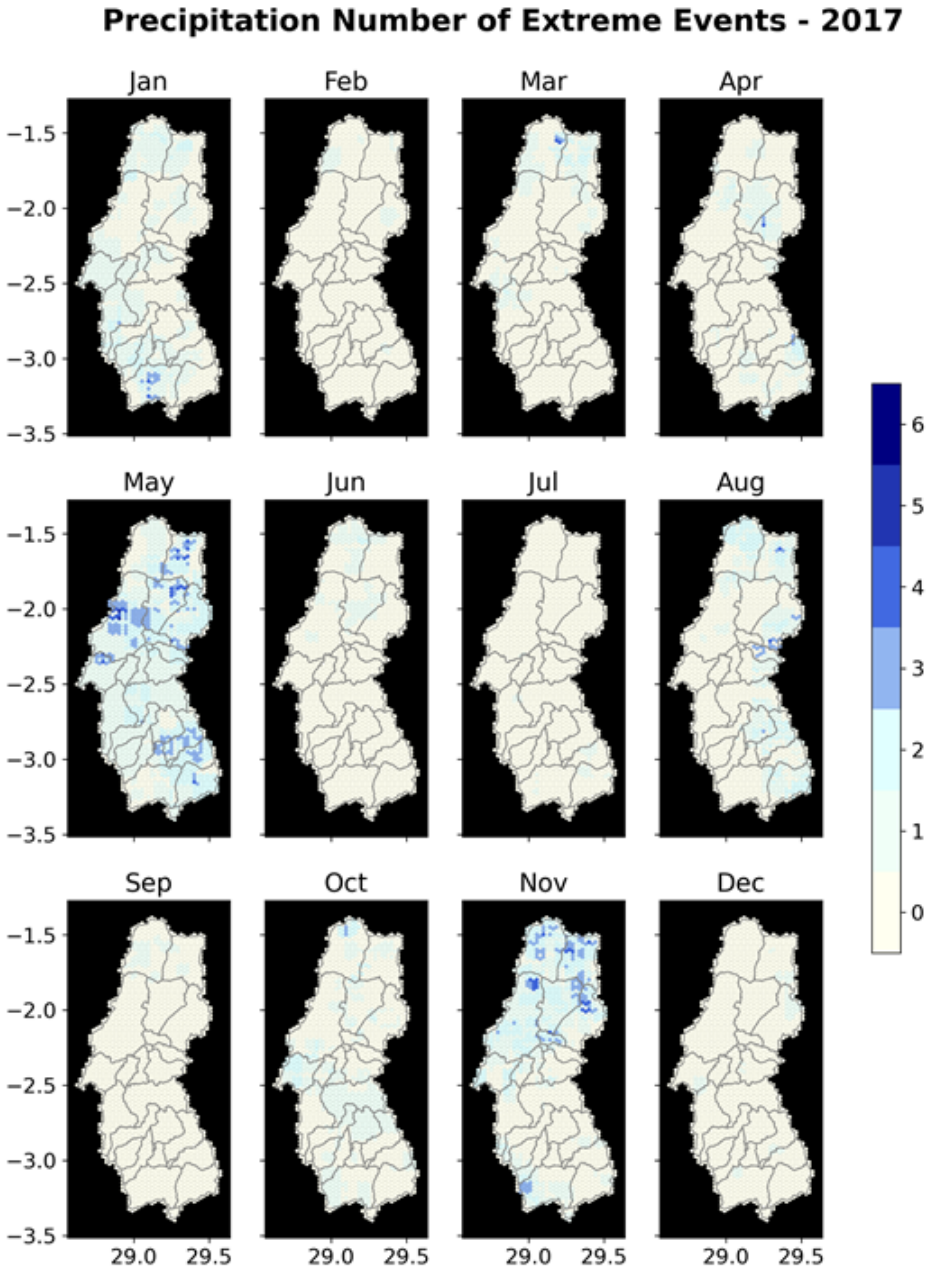

1.5 Mean monthly number of extreme (i.e. above 99-percentile) precipitation events for dry and wet season in 2017.

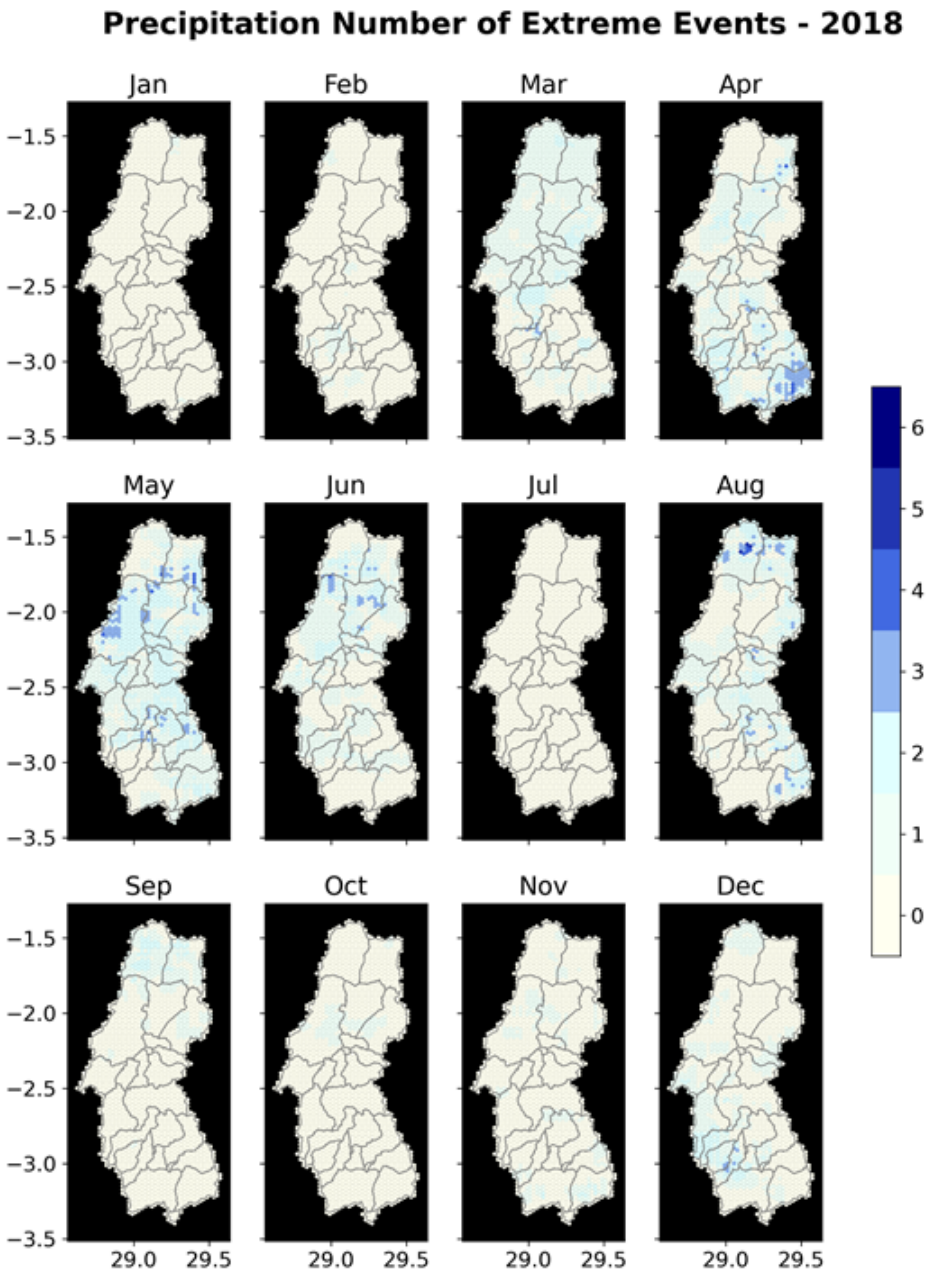

1.6 Mean monthly number of extreme (i.e. above 99-percentile) precipitation events for dry and wet season in 2018.

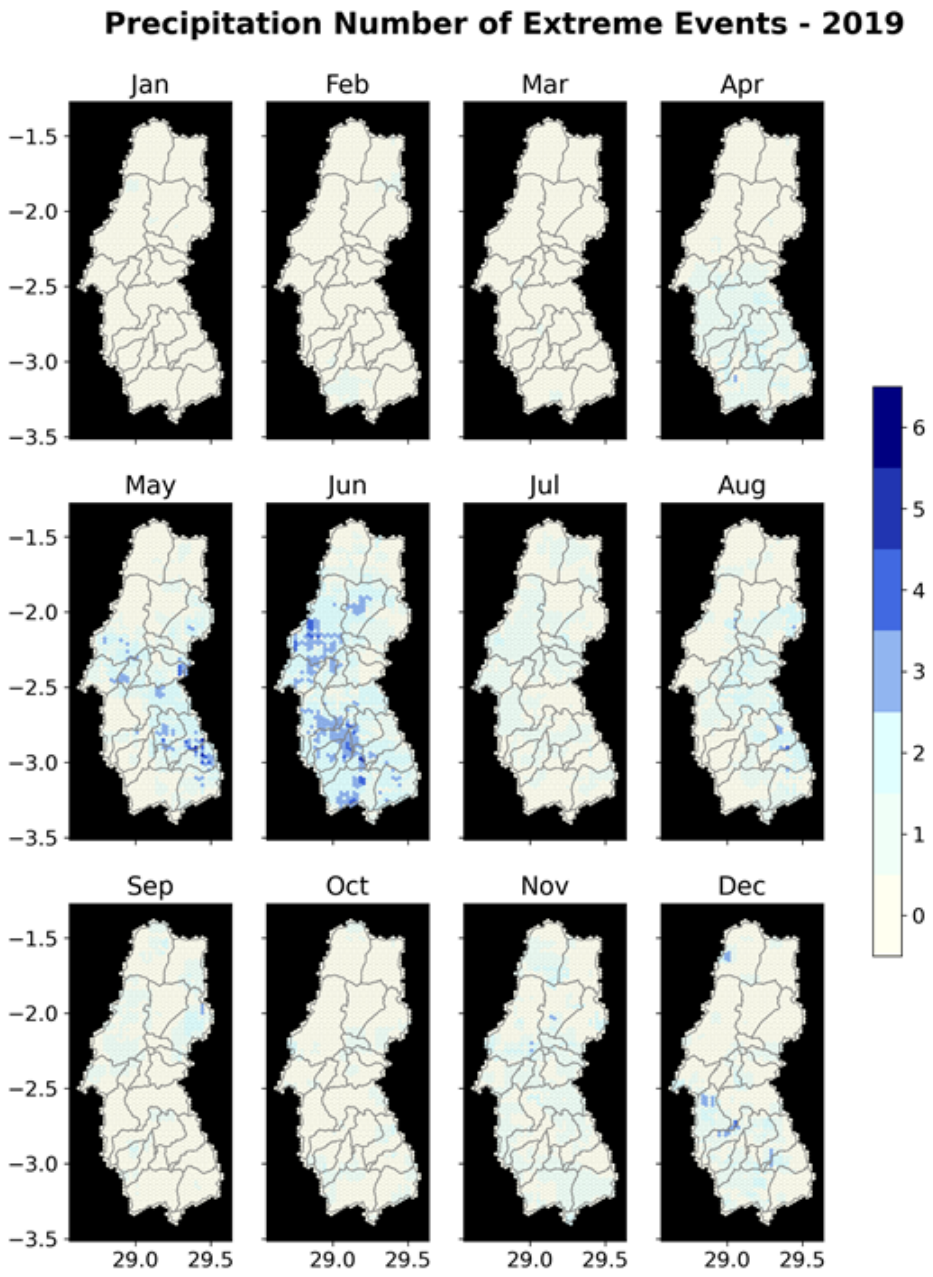

1.7 Mean monthly number of extreme (i.e. above 99-percentile) precipitation events for dry and wet season in 2019.

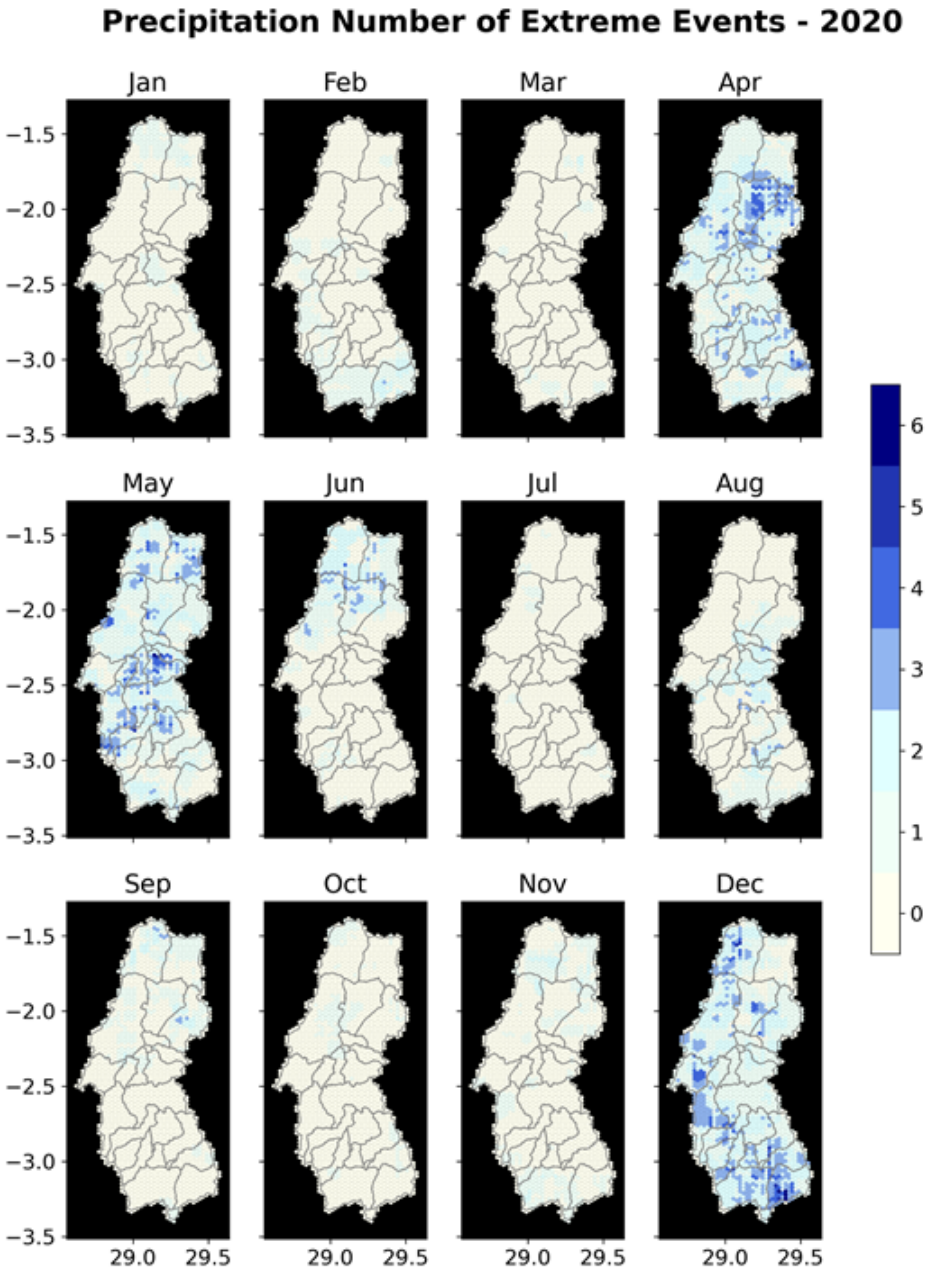

1.8 Mean monthly number of extreme (i.e. above 99-percentile) precipitation events for dry and wet season in 2020.

A.3. Erosion Risk Analysis

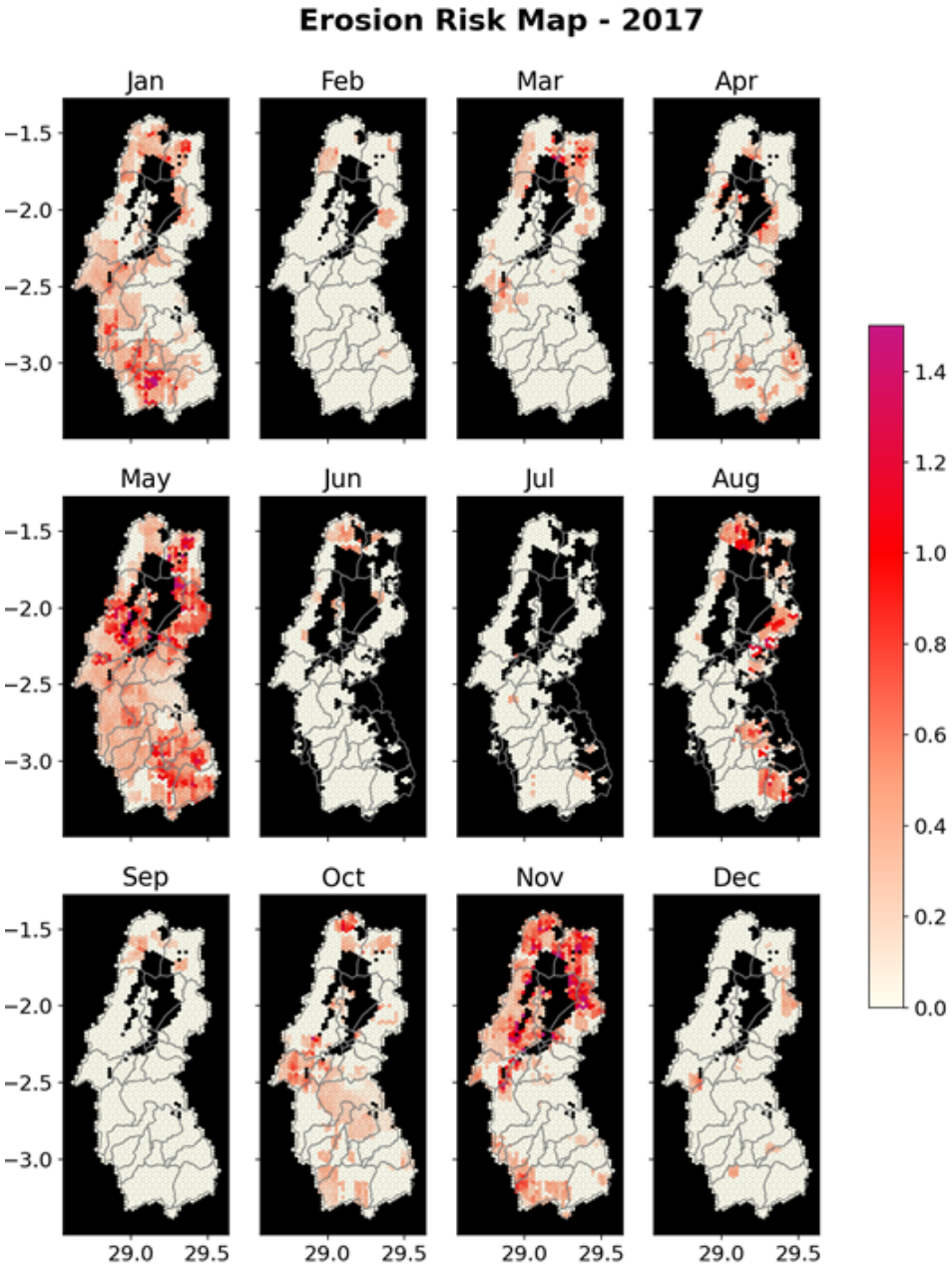

1.9 Erosion risk map derived from the multiplication of NDVI and precipitation for dry and wet season of 2017.

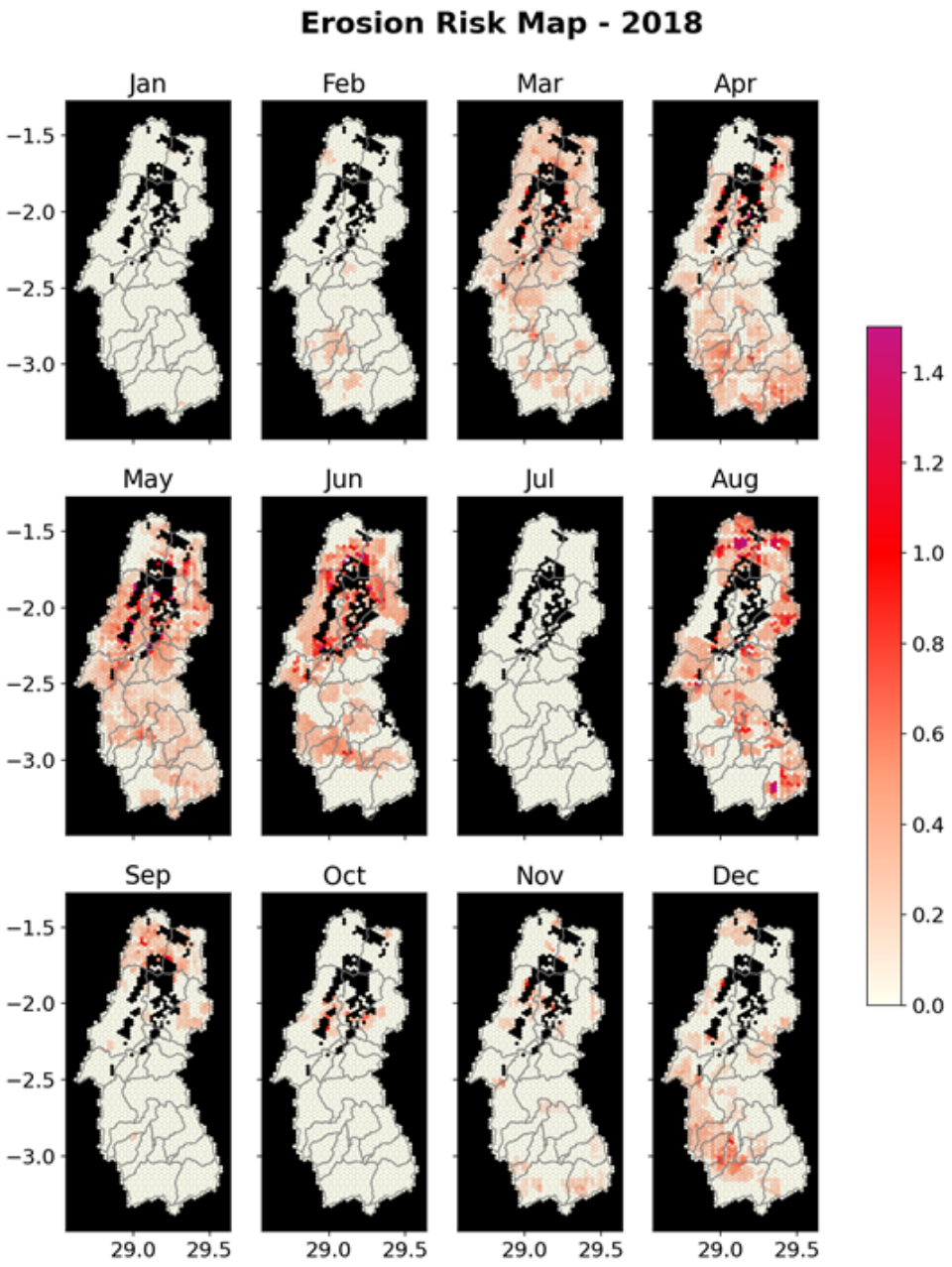

1.10 Erosion risk map derived from the multiplication of NDVI and precipitation for dry and wet season of 2018.

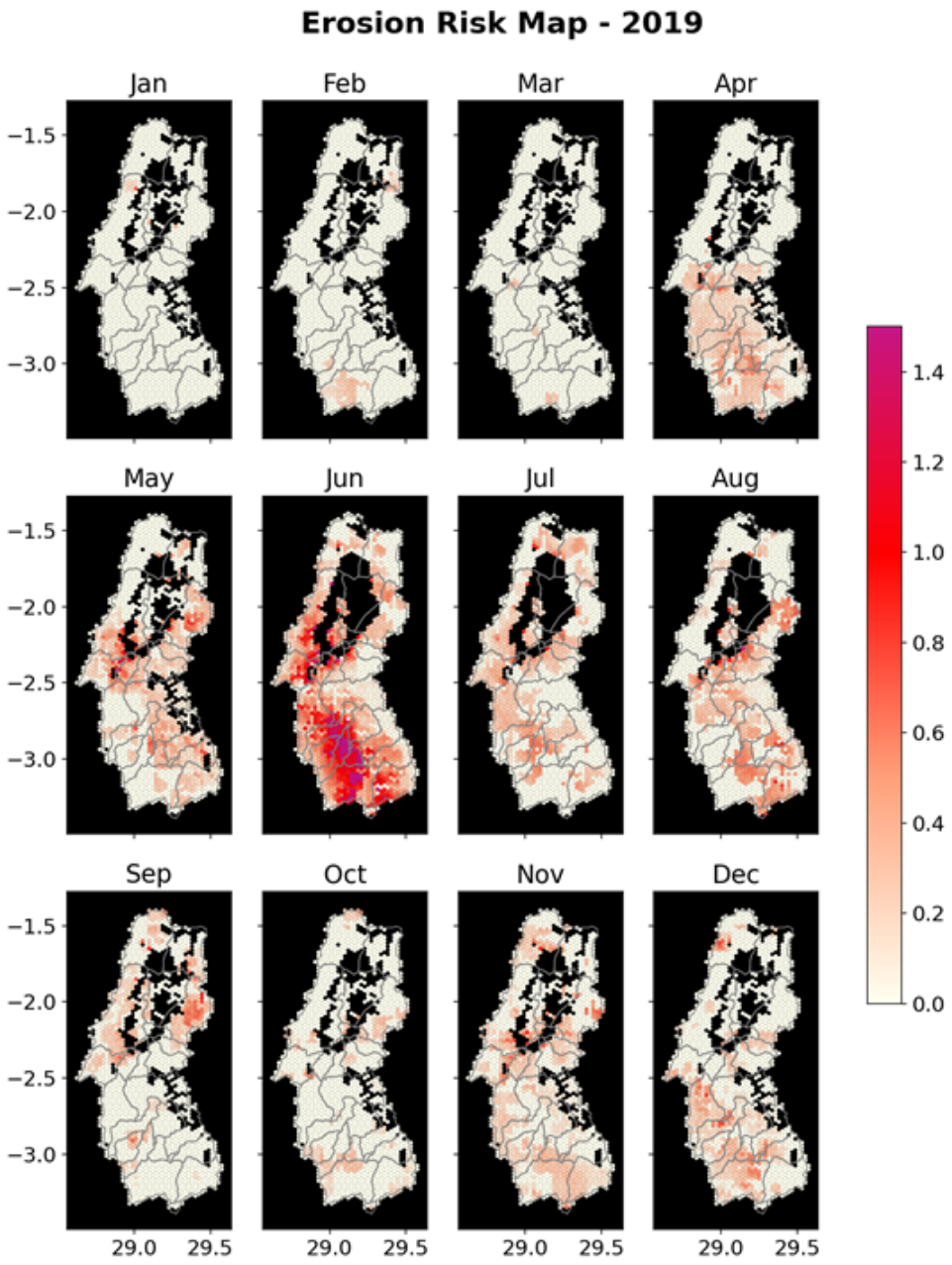

1.11 Erosion risk map derived from the multiplication of NDVI and precipitation for dry and wet season of 2019.

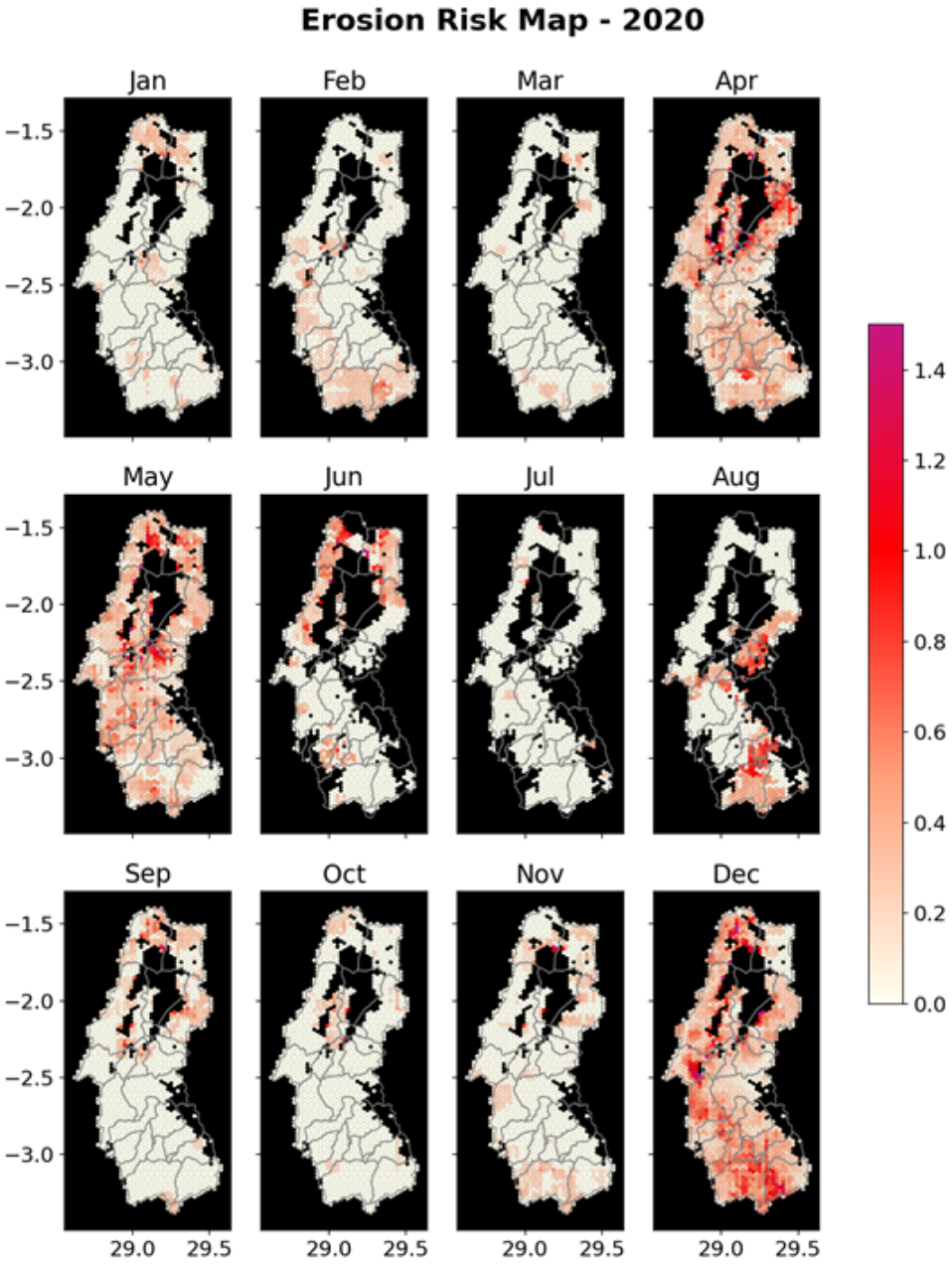

1.12 Erosion risk map derived from the multiplication of NDVI and precipitation for dry and wet season of 2020.

A.4. WP 3: Turbidity Analysis

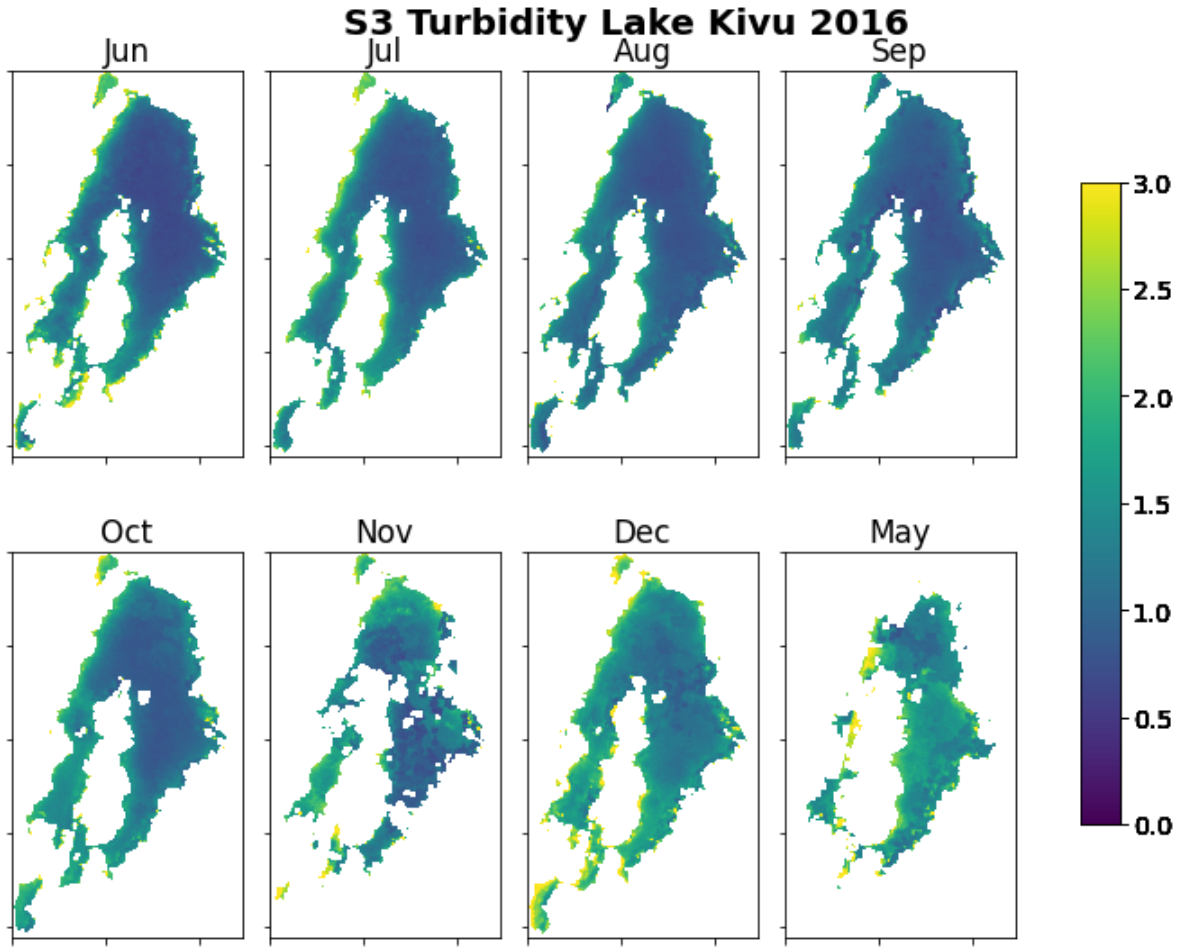

1.13 Monthly mean turbidity of 2017 for lake Kivu based on the CGLS Sentinel-3 turbidity data.

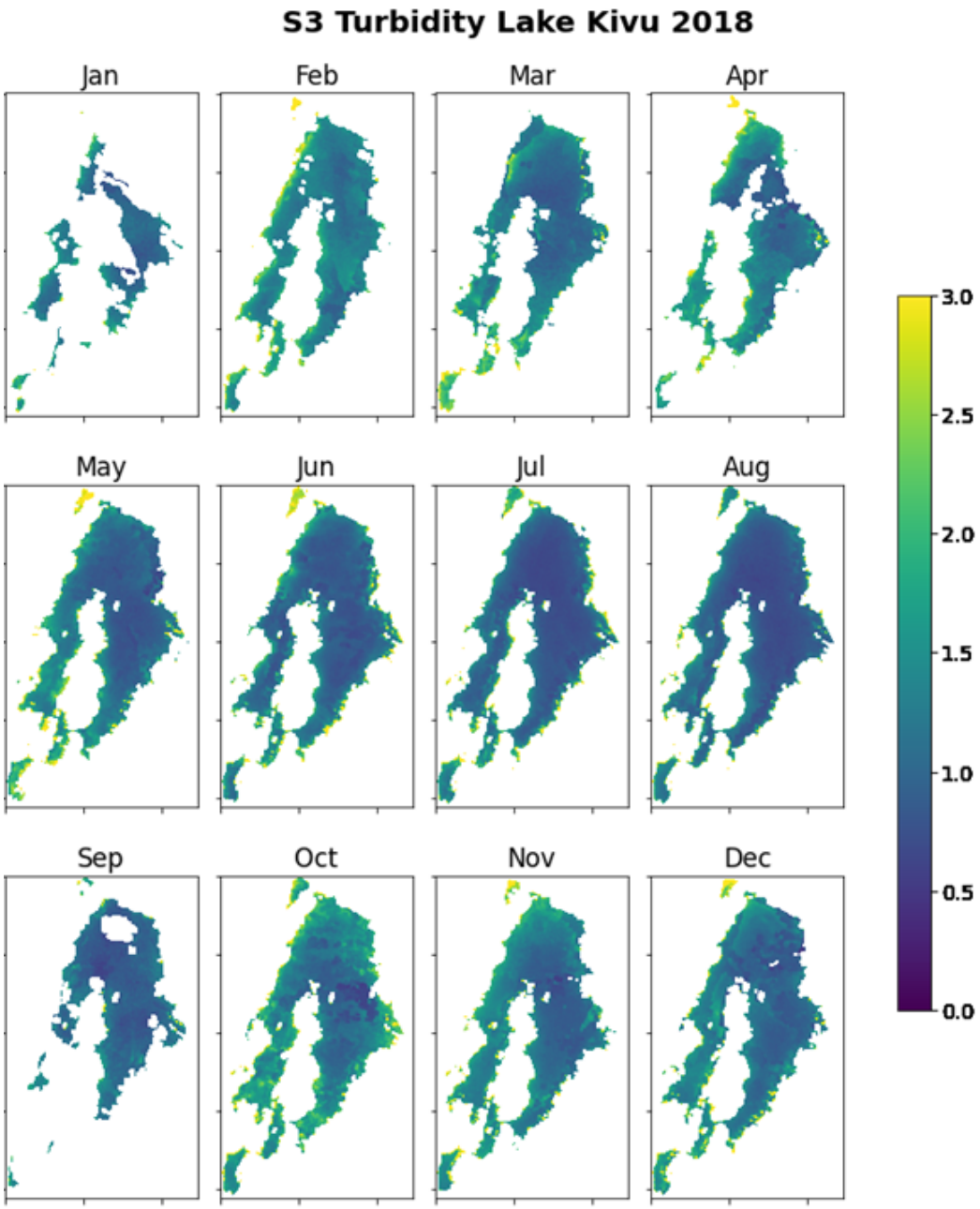

1.14 Monthly mean turbidity of 2018 for lake Kivu based on the CGLS Sentinel-3 turbidity data.

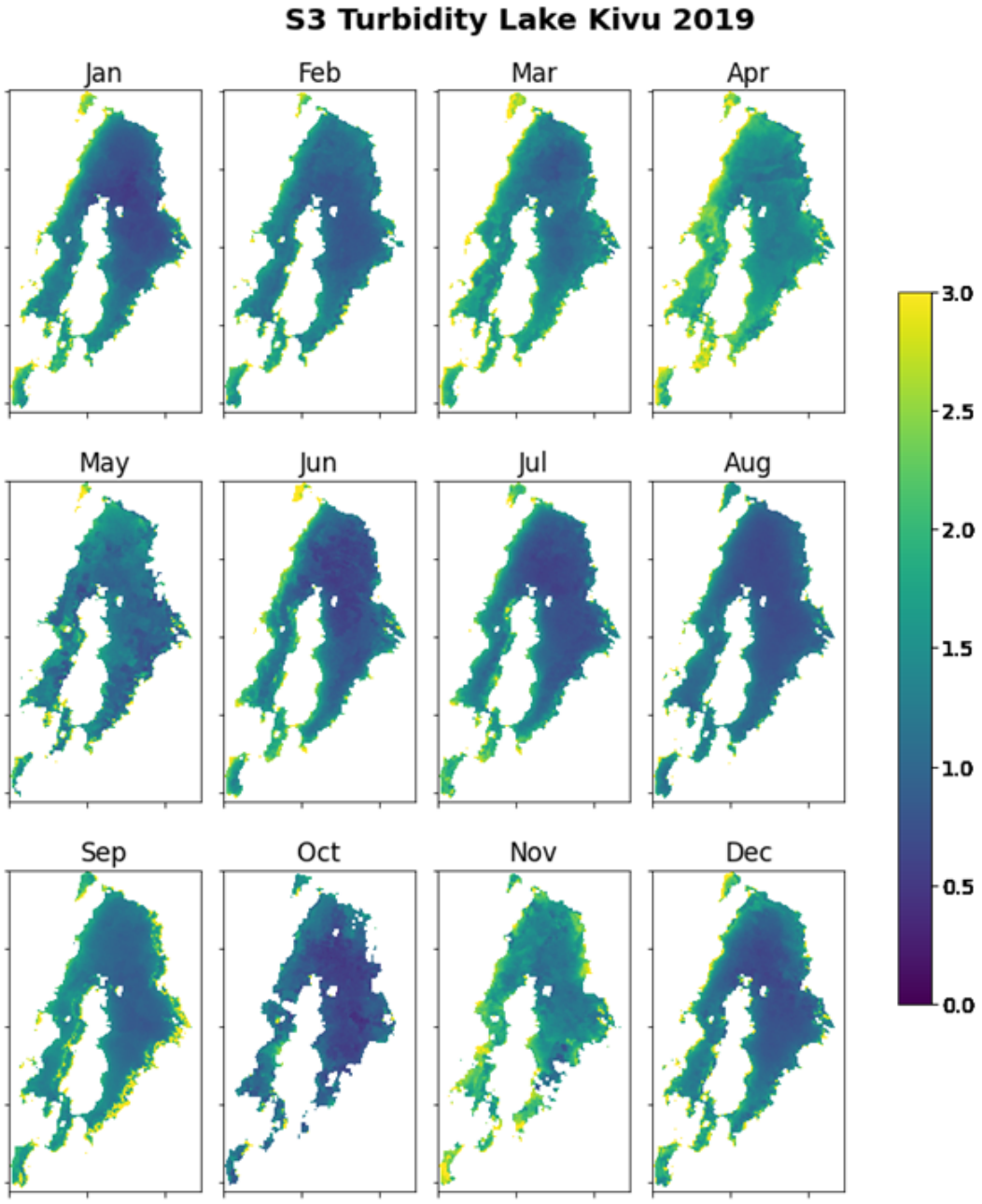

1.15 Monthly mean turbidity of 2019 for lake Kivu based on the CGLS Sentinel-3 turbidity data.

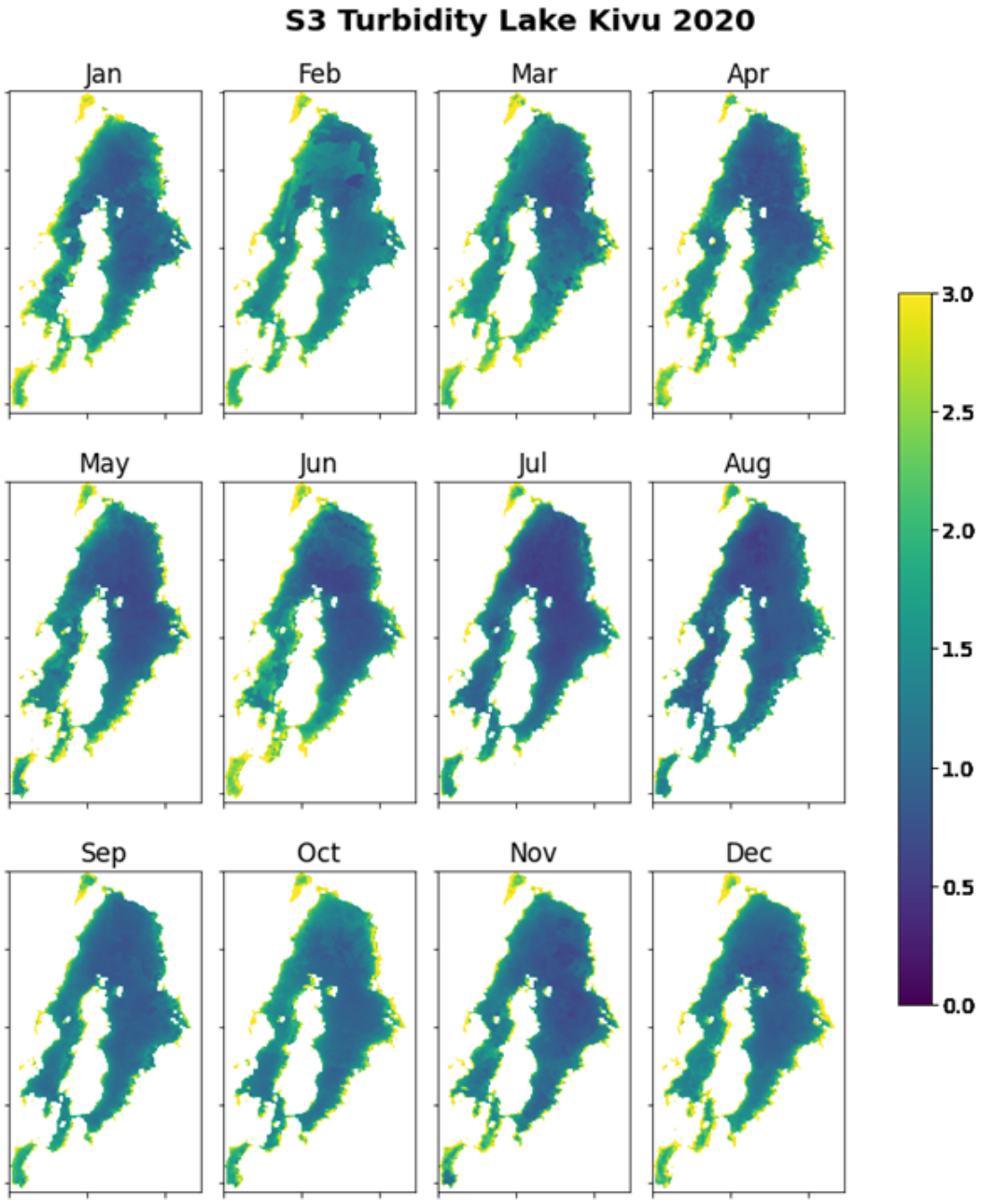

1.16 Monthly mean turbidity of 2020 for lake Kivu based on the CGLS Sentinel-3 turbidity data.

Bibliography

Akayezu, P., L. Musinguzi, V. Natugonza, R. Ogutu-Ohwayo, K. Mwathe, C. Dutton, and M. Manyifika (2020), Using sediment fingerprinting to identify erosion hotspots in a sub-catchment of lake kivu, rwanda.

Borrelli, P., D. Robinson, Fleischer, and L. et al. (2017), An assessment of the global impact of 21st century land use change on soil erosion.

Clarke, K. C. (2017), Improving sleuth calibration with a genetic algorithm, *Proceedings of the 3rd International Conference on Geographical Information Systems Theory, Applications and Management (GISTAM 2017)*, *2*, 319–326, doi:10.5220/0006381203190326.

Clarke, K. C., S. Hoppen, and L. Gaydos (1997), A self-modifying cellular automaton model of historical urbanization in the san francisco bay area, *Environment and Planning B: Planning and Design*, *24*(2), 247–261, doi:10.1068/b240247.

Detsch, F., I. Otte, T. Appelhans, and T. Nauss (2016), A comparative study of cross-product ndvi dynamics in the kilimanjaro region—a matter of sensor, degradation calibration, and significance, *Remote Sensing*, *8*(2), doi:10.3390/rs8020159.

Didan, K. (2021a), *MODIS/Terra Vegetation Indices 16-Day L3 Global 250m SIN Grid V061*.

Didan, K. (2021b), *MODIS/Aqua Vegetation Indices 16-Day L3 Global 250m SIN Grid V061*.

Dietzel, C., and K. Clarke (2007), Toward optimal calibration of the sleuth land use change model, *T. GIS*, *11*, 29–45, doi:10.1111/j.1467-9671.2007.01031.x.

Dinku, T., C. Funk, P. Peterson, R. Maidment, T. Tadesse, H. Gadain, and P. Ceccato (2018), Validation of the chirps satellite rainfall estimates over eastern africa, *Quarterly Journal of the Royal Meteorological Society*, *144*(S1), 292–312, doi:https://doi.org/10.1002/qj.3244.

Eastman, J. R., F. Sangermano, E. A. Machado, J. Rogan, and A. Anyamba (2013), Global trends in seasonality of normalized difference vegetation index (ndvi), 1982–2011, *Remote Sensing*, *5*(10), 4799–4818, doi:10.3390/rs5104799.

FAO and ITPS (2015), The status of the world's soil resources (main report).

Funk, C., P. Peterson, M. Landsfeld, D. Pedreros, J. Verdin, S. Shukla, G. Husak, J. Rowland, L. Harrison, A. Hoell, and J. Michaelsen (2015), The climate hazards infrared precipitation with stations—a new environmental record for monitoring extremes, *Scientific Data*, *2*(150066), doi:10.1038/sdata.2015.66.

Hazarika, M., and H. Kiyoshi (2001), Estimation of soil erosion using remote sensing and gis, its valuation and economic implications on agricultural production, *Sustaining the Global Farm. Selected papers from the 10th International Soil Conservation Organization Meeting held May 24-29, 1999 at Purdue University and the USDA-ARS National Soil Erosion Research Laboratory.*, pp. 1090–1093.

Head, E. M., A. L. Maclean, and S. A. Carn (2013), Mapping lava flows from nyamuragira volcano (1967–2011) with satellite data and automated classification methods, *Geomatics, Natural Hazards and Risk*, *4*(2), 119–144, doi:10.1080/19475705.2012.680503.

Jurasinski, G., and C. Beierkuhnlein (2006), Spatial patterns of biodiversity–assessing vegetation using hexagonal grids, *Biology and Environment-proceedings of The Royal Irish Academy - BIOLOGY ENVIRONMENT*, *106*, 401–411, doi:10.3318/BIOE.2006.106.3.401.

Karamage, F., H. Shao, X. Chen, F. Ndayisaba, L. Nahayo, A. Kayiranga, K. Omifolaji, T. Liu, and C. Zhang (2016), Deforestation effects on soil erosion in the lake kivu basin, d.r. congo-rwanda, *Forests*, *7*, 281, doi:10.3390/f7110281.

Kayiranga, A., A. Kurban, F. Ndayisaba, L. Nahayo, F. Karamage, A. Ablekim, H. Li, and O. Ilniyaz (2016), Monitoring forest cover change and fragmentation using remote sensing and landscape metrics in nyungwe-kibira park, *Journal of Geoscience and Environment Protection*, *04*, 13–33, doi:10.4236/gep.2016.411003.

La, H. (2013), Analysis of the relationship between modis ndvi, lai and rainfall in the forest region of rwanda, *International Journal of Digital Content Technology and its Applications*, *7*, 559–569.

Landmann, T., and O. Dubovyk (2014), Spatial analysis of human-induced vegetation productivity decline over eastern africa using a decade (2001–2011) of medium resolution modis time-series data, *International Journal of Applied Earth Observation and Geoinformation*, *33*, 76–82, doi:https://doi.org/10.1016/j.jag.2014.04.020.

Lehner, B., and G. Grill (2013), Global river hydrography and network routing: baseline data and new approaches to study the world's large river systems, *Hydrological Processes*, *27*(15), 2171–2186.

Marconcini, M., A. Metz-Marconcini, S. Üreyen, D. Palacios-Lopez, W. Hanke1, F. Bachofer, J. Zeidler, T. Esch, N. Gorelick, A. Kakarla, M. Paganini, and E. Strano (2020), Outlining where humans live, the world settlement footprint 2015., *Scientific Data*, *7*(242), doi:10.1038/s41597-020-00580-5.

Musau, J., S. Patil, J. Sheffield, and M. Marshall (2018), Vegetation dynamics and responses to climate anomalies in east africa, *Earth System Dynamics Discussions*, *2018*, 1–27, doi:10.5194/esd-2017-123.

AUTORITE DU BASSIN DU LAC KIVU ET DE LA RIVIERE RUZIZI
ABAKIR

Immeuble de la CEPGL
GISENYI / RUBAVU - RWANDA
info@abakir.org

www.abakir.org